Time in which the forecast from the GCM is calculated (UT)	forecast (hours)
12:00 of day (J-2)	30
12:00 of day (J-2)	36
12:00 of day (J-2)	42
12:00 of day (J-2)	48

Table 107: Initialization and forcing data to be used for Meso-Nh simulations in operational configuration for forecasts of the night J with results to be ready at 14:00 LT of the day (J-1).

8 Work Package 3.2 - Initialization and forcing data

8.1 Source/dealer, data costs and procurement, modality of data delivery

The forecasts products produced by the ECMWF General Circulation Model (GCM) with a different frequency depending of the product itself are then distributed to the different meteorological national services. After a detailed investigation we identified the European Center for Medium Range Weather Forecast (ECMWF) as the most suitable dealer for the data to be used to initialize and force the simulations performed with the mesoscale model Meso-Nh. The criteria we considered for the dealer selection was mainly the cost of the products/service of delivery, the conditions that the dealer can assure to deliver the products (such as delay time with respect to the GCM delivery). Due to the fact that ESO is an international organization it has the access to all the ECMWF data we require for free (as prescribed by ECMWF rules). A detailed request of the input data for nightly simulation at Cerro Paranal and Cerro Armazones that we intend to perform has already been given to ESO (at the beginning of the 2015 solar year). ESO already provided to submit the request to the ECMWF and, since spring time of 2015, the initialization and forcing data are daily delivered to ESO by the ECMWF. We note that, in perspective, following the rules of the ECMWF, it will be possible to ask for modification of the list of parameters if we will judge the necessity to add other products. Another important element to take into account is that the web page related to the nightly predictions that the MOSE team will performed has to be protected therefore accessible only to ESO and the MOSE team.

For the initialization and forcing data we identified as a suitable surface $\sim 14°$x$14°$ around the site of interest. These data cover the volume defined by the surface ($14°$x$14°$) and the height of the GCM model. From the 25 June 2013 (Cycle 36r1) the GCM model has 137 vertical levels reaching the top model level of 0.01 hPa. The horizontal resolution of initialization and forcing data is at present 0.125 degrees corresponding to roughly 16 km (T1279). This information is contained/saved in files in GRIB format. Tests have been done to check that initialization data on GRIB files limited to such a sub-domain provide the same result obtained with a GRIB file extended on the whole Earth. This proves that the selected configuration is suitable for our application. Table 107 reports the initialization and forcing data set. Due to the fact that the simulations will be performed in Florence, we will retrieve daily via ftp from ESO the initialization and forcing data.

8.2 Data access and third party rights

The MOSE team can use these data only and exclusively to produce the forecast in the context of the MOSE project/contract (see Rules governing the distribution and dissemination of the ECMWF real-time products). As highlighted previously, the web page with the outpus of the predictions performed with the Astro-Meso-Nh code will be protected by a password. Starting from version 5.1, Meso-NH is freely available under CeCILL-C license agreement that is available at the Meso-Nh web page $http://mesonh.aero.obs-mip.fr/mesonh51$. However, considering that we are dealing about a service that the MOSE team provides to ESO, all kind of constraint refers to the MOSE team (not to ESO). The Astro-Meso-Nh code is property of INAF-Arcetri but this has no impact on the demonstrator because the MOSE Team provides a service to ESO and machines are not locally placed at ESO.

9 Work Package 3.3 - End-to-end process plan

9.1 Introduction

During the MOSE Phase B we (INAF-Arcetri for MOSE team) undersigned a convention with the Italian laboratory 'Laboratorio di Monitoraggio e Modellistica Ambientale' (LAMMA), a public consortium between the Italian National Research Council (CNR) and the Italian Tuscany Region (located in Florence too) with the aim to set-up a collaboration between the MOSE team (Arcetri-INAF) and LAMMA to manage forecasts of the optical turbulence and atmospherical parameters for international astronomical observatories. The idea behind such a joint venture is that, joining our different expertise, we can provide directly the service to different astronomical observatories in the world[6]. This solution is an alternative to the original plan figured out at the beginning of MOSE-Phase B (and discussed with the MOSE ESO-Board) that was to provide a self-consistent system to ESO and to offer an external support made by the MOSE team. The advantages for the 'service solution' are several for both ESO and the MOSE-team. From our side, under this configuration we should be in the condition to provide the service to several observatories supported by colleagues with expertise in managing operational weather forecasts. We can operate directly in situ for whatever problem. We also by-pass whatever complications due to copyright of our Astro-Meso-Nh package. Since we intend to offer this service to different Observatories we prefer to keep at home the code. In an extreme synthesis, Arcetri should take care of the scientific development of the turbulence forecasts for ground-based astronomy, automation of the system, up-dating of the code, analysis and up-dating of the model performances. LAMMA will guarantee the provision of the operational service from the downloading of the initialization data to the simulation run and the product delivery on the dedicated web pages, according to what will be the contract specification (including the daily notes on the web page about the atmospherical predictions if requested). The advantage for ESO is that they do not have to take care about the forecast system, the system can be more easily up-dated if this is necessary to obtain the most performant and useful outputs and the work should be done by competent man power.

In occasion of a MOSE review that took place on 19 May 2015 in Garching this option has been discussed with the ESO Board and the Board expressed its interest for this solution. We agreed with ESO that, after the MOSE Final Review, we would have started the negotiation. Our intention for the budget is to proceed in the terms described here. The costs for ESO would include a set-up expenditures (hardware, all fixed costs to set up the system) associated to the two sites of Paranal and Armazones plus an operating expenditure related to the service offered. We highlight that all the servers are dedicated. This means that each server is used only for the specific project/site. This is a condition intrinsically necessary for the project itself. In the document E-TRE-INA-245-0010.1 details on the costs will be provided.

9.2 Baseline scheme

A preliminary overview of the forecasts plan has been presented in the MOSE Report - Phase A (Section 8). In the Introduction of MOSE Report - Phase A a simple toy model describing how an OT forecast works has been presented (Section 1.3 - Fig.2). Besides, a general description of the elements necessary to perform the OT forecast and a complete sequence of processes necessary to perform the OT forecast has been included (MOSE Report - Phase A, Section 8). In Phase B we provided a more detailed plan (see Fig.67). We repeat here briefly the main steps already described in Phase A to permit to the reader to better follow the main steps. From an operational point of view, the mandatory steps to perform a real-time OT forecasts at an ESO site are summarized in the scheme of Fig. 70.

As soon as the GCM (in our case, the ECMWF) makes available the meteorological files coming from its real-time global forecasts (T+12h, T+18h, T+24h, T+36h, T+48h, etc.), these files are sent to the contractor

[6]LAMMA has expertise in operational weather forecasts. It is taking care of the weather forecasts performed on a regional scale for the Italian Tuscany Region. These weather forecasts are used by the Tuscany Region for several different applications such as civil protection, quality of air, etc...

(ESO) through ftp. This is done with a fixed and guaranteed delay time. Arcetri/LAMMA team will retrieve at a fixed and guaranteed daily frequency the data through ftp from the ESO repository.

Automatic daily procedures (using for example bash scripts and crontab) will then copy these files onto the local workstation (or cluster, or super-computer...) where the Meso-NH model is installed and ready to perform the OT forecast (**step (1)** of Fig. 70). Immediately after the end of the transfers, the preparation of the simulation can begin (it consists in creating the initialization and coupling files for the given night). Once the files created, the Meso-NH simulation itself (the OT forecast) can start (this is **step (2)** of Fig. 70). At the end of the simulation, the Meso-NH outputs are post-processed (diagnostics computed using Fortran and idl procedures, **step (3)** of Fig. 70) in order to generate figures including predicted parameters to be displayed on a dedicated web-page freely accessible by astronomers, instruments scientists, etc....(**step (4)** of Fig. 70).

All these steps are part of an automated process that we have to implement through bash scripts and crontab on a Linux machine.

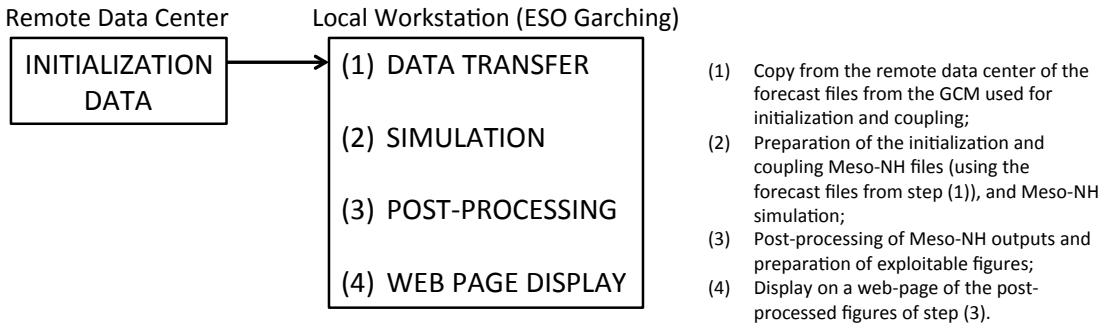

Figure 70: Operational forecast system overview.

The general end-to-end operational system scheme is shown in Fig.71. The ECMWF delivers daily the initialization (and forcing) data to ESO. From Florence, where the High Performance Computing (HPC) facilities are located and the Astro-Meso-Nh code is installed, we retrieve daily the data through ftp. The simulation is performed in Florence. The outputs of the simulations are treated in the post-processing phase and go the Web Server that is accessible through the net by ESO and the Arcetri/LAMMA Team. In a repository (NAS Data Server) part of the raw outputs of the simulations is stored. Another part is simply discarded.
In Fig.72 is shown a more detailed scheme of the system in which the two network systems (red lines) are put in evidence: the main network and a back-up network that can work in case of a temporary failure of the main network. Data provided by ECMWF are delivered to ESO. In case of a failure on the ECMWF-ESO network connection, data are delivered to the back-up site (a back-up IP address is in general requested by ECMWF to the client - to be discussed that with the Board in occasion of the Final Review). The selected HPC facilities (see Section 7) will be located in the Center for Elaboration Data (CED) of LAMMA. Initialization and forcing data are retrieved from the ESO repository to LAMMA through ftp and the procedure of simulation starts. This procedure is done by two steps: (1) a coupling of Meso-Nh with the orography (Digital Elevation Model) and the initialization and forcing data and (2) the real Meso-Nh simulation covering a whole night. When the simulation is completed the model outputs are stored in a NAS Data Server (only a part of them are stored). At the same time, in the HPC facilities the post-processing phase starts producing the outputs to be stored on the Web Server. Each day, the new outputs are refreshed on the Web Site. In our first baseline we planned to include the option to look at the forecast outputs of the night before too (the option can be discarded if ESO is not interested on that). In Section 7.3 are reported the totality of the stored data.

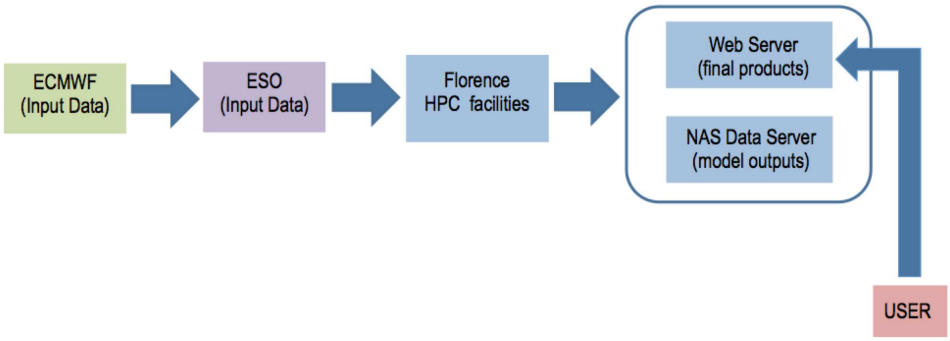

Figure 71: General end-to-end operational system scheme.

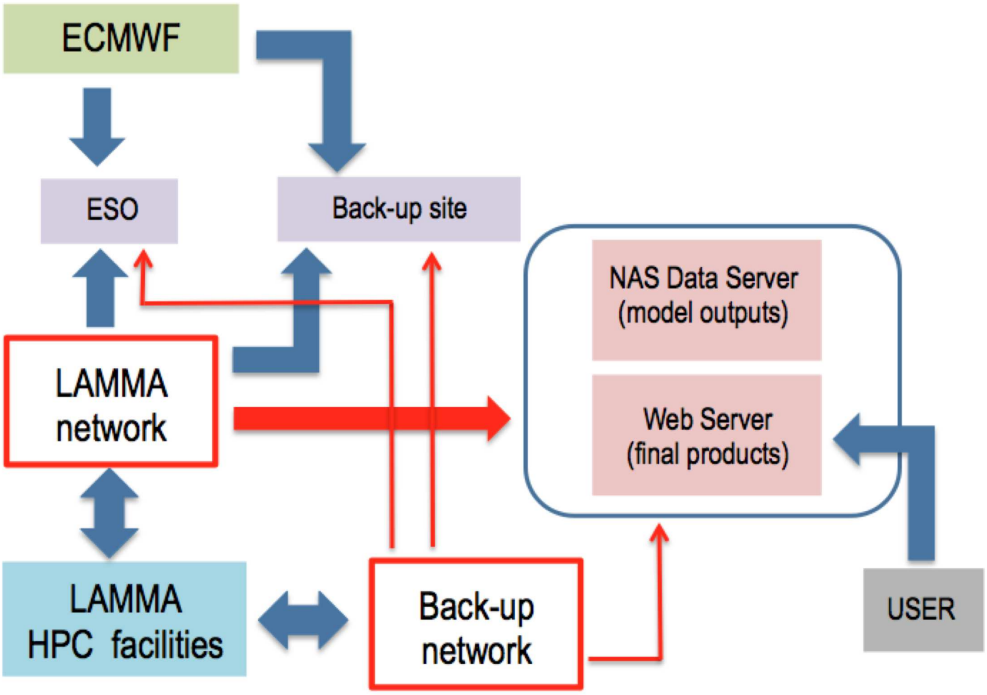

Figure 72: Detailed scheme including the standard and back-up networks (red lines).

10 Conclusions

We summarize here the main conclusions we achieved in terms of the performances of the Meso-Nh and Astro-Meso-Nh model in reconstructing the atmospherical parameters relevant for the ground-based astronomy and the astro-climatic parameters.
The main goal of this feasibility study was to establish if the model in the present form was able to provide a sufficiently high level of performances in order to produce a benefit in terms of the Service Mode of the VLT and the E-ELT.
We went well above our expectations and we could prove, using different statistical operators, that this scientific tool is able, just now, to provide a concrete added value to the Service Mode and it can provide fundamental informations in a number of different contexts not only related to the forecast of the astro-climatic parameters. Among these other contexts we cite the forecast of the temperature close to the ground to thermalise the dome at the beginning of the night; the forecast of the wind speed and direction fundamental to prevent vibrations on facilities supported by AO systems; the forecast of the wind speed vertical profiles that can be used not only to forecast the τ_0 but also to estimate the τ_0 in real-time joint to the C_N^2 coming from instruments dedicated to the OT measurements, the use of the forecast not only for the prediction but also as an input of AO systems (see [56]), etc.). The feasibility study and the discussions we had with the ESO Board permitted us to conceive a number of figures of merit that can represent the base for the use of this tool by the resident astronomers during each night. Equally interesting are the potentialities we put in evidence for further developments of this tool. For example, the testing of a new algorithm for the C_N^2 indicates the possibility to forecast reliable C_N^2 profiles with a vertical resolution up to 150 m. This might be a invaluable support for the implementation of the most sophisticated AO techniques such as MCAO and MOAO.
In most cases, the model presents, just now, excellent performances. In few cases, the model shows good performances even if there is still space for improvements. In all cases however, the positive impact and added value in many different contexts of the ground-based astronomy, particularly that assisted by AO (included the WFAO), is evident.

10.1 Atmospherical parameters

We summarize here the results concerning the atmospherical parameters relevant for the ground-based astronomy. For **Cerro Paranal** we performed an extended statistical study on the model performances in reconstructing the temperature, the wind speed and direction and the relative humidity **close to the ground** on a sample of 129 night uniformly distributed in three years: 2007, 2010 and 2011. A set of statistical operators have been used to quantify the model performances: the bias, the RMSE, the σ and, from the contingency tables, the percent of correct detections (PC) and the probability of a correct detection (POD_i) in specific ranges of values. On the same sample of 129 nights we tested the model performances using, as a initialisation and forcing data, the analyses and the forecasts from the ECMWF. The set of forecasts are the same we should use in an operational configuration. The goal of the study was to quantify how much (and if) the quality of the forecasts obtained with the mesoscale model decreases using the ECMWF forecast instead of the ECMWF analyses as initialization data. Here the results that we obtained in a nutshell:

- **Temperature -** The percent of correct detection PC computed from a 3×3 contingency table (having as a threshold the climatological first and third tertiles calculated on a few years) is excellent. It is of the order of 77% with slightly small differences depending on the height (2 m or 30 m). PODs are mostly larger than 66%. The best POD is 93.7% at 30 m for the temperature inferior of 11.5°C. At every levels, the extremely bad detection (EBD) is almost equal to 0%. In all cases PC and PODs are well larger than the random case (33%). The bias (simulation minus observation) is as small as -0.12°C and -0.37°C at 2 m and 30 m. The σ is equal to 0.99°C and 0.94°C at 2 m and 30 m a.g.l. The RMSE is equal to 0.99°C and 1.02°C at 2 m and 30 m a.g.l. The median value on individual nights of σ is 0.54°C and 0.48°C at 2 m and 30 m. No major differences have been observed in winter and summer time. Just a slightly larger σ and smaller bias in summer.

- **Wind speed -** The percent of correct detection PC computed from a 3×3 contingency table (having as a threshold the climatological first and third tertiles calculated on a few years) is very good (around 60% when the highest horizontal resolution ΔX=100 m is used). The probability to detect the wind velocity in the three sub-samples limited by the tertiles of the cumulative distribution is good too. The strongest wind is especially well detected by the model: POD_3 is equal to 74% (at 10 m) and is equal to 79% (at 30 m). In all cases the PC and the POD are greater than 33%, typical value for a random distribution. We also proved that the configuration with the horizontal resolution of 100 m in the innermost domain provides a much better model performances in reconstructing strong wind speed mainly because the digital elevation model (DEM) better matches with the real orography and the interactions of the atmosphere with the ground almost eliminates the underestimation of the wind speed observed with the model at 2 m and ΔX=500 m. With ΔX=100 m the bias (simulations minus observations) is -1.16 ms^{-1} and -0.24 ms^{-1} at 10 m and 30 m. The σ is 2.47 ms^{-1} and 2.69 ms^{-1} at 10 m and 30 m. The median value on individual nights of σ is 1.25 ms^{-1} and 1.45 ms^{-1} at 10 m and 30 m. No major differences have been observed in winter and summer time.
- **Wind direction -** Differently from the temperature and the wind speed, we have analyzed 4×4 contingency tables. If we consider the separation in the four categories (NE, SE, SW, NW), the PC is 67.5%. If we consider the separation in the four categories (N, E, S, W), the PC is 77.7%. Both values are much better than for a random forecast (PC=25%) of a 4×4 contingency table. The POD of the wind is very good in the quadrants from which the wind flows more frequently (N and NE) with PODs of the order of 92.8% (N) and 81.7% (NE). The POD is not satisfactory (∼ 27%) only in the narrow angular sector [225°, 270°]. However the occurrence of wind blowing from SW is the less probable (only 4% of the time for the observed sample of 129 nights). The impact of the model performances on this case can be considered therefore negligible. The bias is 9.36° and 5.02° at 10 m and 30 m. The RMSE is equal to the σ and is 36.5 ° and 35.7 ° at 10 m and 30 m corresponding to $RMSE_{rel}$=20.4 % and 19.8% at 10 m and 30 m.The median value on individual nights of σ is 11.12 ° and 10.11 ° at 10 m and 30 m. No major differences have been observed in winter and summer time. Just a slightly larger σ and smaller bias in summer.
- **Relative humidity:** the RH has been treated in a slightly different way. We added to the sample of 129 nights further 13 nights in which the observed RH was particularly high (> 70%). This happens very rarely (only a few nights) during each solar year. In this region indeed, the RH is extremely low (median value of the order of 10%). It is therefore not really interesting to forecast the RH but it would be useful to identify the few nights during each year having a high value of RH. Results indicate that the model well discriminate the nights with low (< 30%) and high (> 60%) value of RH (POD_1=75.2%, POD_3=71.2% and POD_3=71.7%). However it shows a tendency in overestimating the low values of the RH and in slightly underestimating the high values. Example: an observed RH of 10% can be seen by the model as 20-25% and an observed RH of 80% can be seen by the model as 65-70%. The first issue is of no interest from the point of view of the astronomical observations. The second issue tells us that the model can easily reconstruct a RH > 60%, however, it is more difficult to discriminate between strong values (for example 70% and 90%). Besides that we observe that all the 13 nights in which the observed RH was very high (order of 80%), the model reconstructed RH > than 60% (see Fig.A3 and A4 in Lascaux et al. 2015[53]). From a practical point of view this simply implies that the resident astronomers should take as critical all the conditions in which RH is > 60 % because it can be that, in a few cases, the RH overcomes the threshold of 80% (threshold of closure of the dome).

We think there is still space for improvement of the bias and RMSE (not σ) using the multiplicative coefficients as we did for the contingency tables. **Using the ECMWF forecast as initialization and forcing data, the results are almost the same and the model looses just a few percent or it presents the same performances**. The reader can find the details in Session 3. A few further results, obtained using the ECMWF forecasts as initialisation and forcing data, are worth to be reported here.

Wind direction forecast under strong wind speed conditions (WS > 12 ms^{-1})

The contingency table 3×3 and PC and PODs tell us that the model performances in reconstructing the

wind flowing from the North-East (NE) is excellent (> 90%) even better for the wind direction at 10 m. This is also the sector in which the wind speed is more frequent. The model has also an excellent behavior (100%) in reconstructing the wind direction from the South-East (SE) also if it is not so frequent that wind flows from this direction when the wind speed is > 12 ms^{-1}. The POD(NW) is equal to 71.1% (at 10 m) and 56.4% (at 30 m) that is still very good even if slightly inferior with respect to the previous cases. To conclude, the model correctly do not reconstruct wind direction flowing from the SW. The wind direction basically never flows from this direction.

Trend of the wind speed

We divided the night ($\sim$ 9 hours) in 3 and 5 sectors. We considered intervals of 180 minutes (i.e. 9 hours divided by N=3) and 108 minutes (i.e. 9 hours divided by N=5). Then we consider two different discretization of the trends: **(A)** in the first case we discriminate between positive and negative trend i.e. when the jump of the wind Δ_{mnh} is > or < 0 passing by a sector to the contiguous; **(B)** in the second case we discriminate between a positive, a stable and a negative trend. The 'stable' condition is defined when the jump of the wind Δ_{mnh} is included in the range [Δ_{lim1}, Δ_{lim2}]. We used as Δ_{lim1} and Δ_{lim2} the median values of Δ. Case (A) gives very good results with PODs between 55.6% and 83.2% (for N=3). For N-5 the PODs are slightly lower (between 52.5% and 72.9%. Case (B) provides more modest (but still good) performances with PODs included between 43.3% and 66%. We also tried to use a percentage of the ratio of the wind speed in the interval T and T+1 achieving substantial similar results.

For **Cerro Armazones** we performed a similar study aiming to validate the model performances in reconstructing the atmospherical parameters close to the ground using, as initialization and forcing data, the ECMWF analyses. We have been forced to use two different samples of 42 and 53 nights because TMT and ESO instrumentation has been used in different years. We refer the reader to Section 1.2.1 and Section 1.3.1 for the details. The most relevant outputs can be summarized in: (1) results obtained with the instrumentation of TMT and ESO are comparable and (2) results obtained at Armazones are in general as good as Paranal.

For what concerns the model performances in reconstructing **the vertical profiles of the temperature, wind speed and direction extended on the whole 20 km** we refer the reader to the papers Masciadri et al., 2013 [51], discussed in Phase A. In a most recent paper Masciadri et al. 2015 [57] we proved (see Fig.1) to be able to improve the model performances in reconstructing the wind direction in the low part of the atmosphere filtering out all measurements in which the wind speed is $\leq$ 3 ms^{-1}. The validation of the model in reconstructing the vertical stratification of the atmospherical parameters has been done comparing the Meso-Nh model outputs with observations from 53 radio-soundings distributed in summer and winter (2009) above Cerro Paranal. The great accuracy of the model has been observed not only in statistical terms but also on all the individual vertical profiles. Such an excellent performances permitted us to use this tool as a reference to validate the wind speed retrieved from GeMS ([56]). In that preliminary study done on 11 nights we proved that GeMS in many cases provides excellent estimates of the wind speed but, at the same time, we proved that, in a some cases, the error is not negligible. The simultaneous use of Meso-Nh and GeMS can therefore improve the estimations of the wind speed and the C_N^2 from GeMS (and whatever MCAO system). The goal of a forthcoming paper will be to enrich the statistics ($\sim$ 40 nights).

10.2 Optical Turbulence

The most important result obtained in Phase B has been the modification of the algorithm of the C_N^2 that definitely improved the model performances and solved the problem of the weak temporal variability of the optical turbulence in the free atmosphere. We analyzed the three main integrated astro-climatic parameters as originally planned: seeing (ε), isoplanatic angle (θ_0) and wavefront coherence time (τ_0). The Astro-Meso-Nh model has been first calibrated using measurements done with a Generalized SCIDAR. The model performances have been quantified using independent samples of nights. The results we obtained on the validation samples

are summarized in a nutshell:

- The **wavefront coherence time (τ_0)** is the parameter that, at present time, is predicted with the best score of success. All the POD_i (i = 1, 2 and 3) are satisfactory and comparable to those obtained among different instruments, in some cases even better. From a scientific point of view, the most interesting POD for τ_0 is POD_3 that is the probability to detect a τ_0 larger than the third tertile. **POD_3 on the validation sample is included in the range [72% - 78%] if we considered the most reliable instrument as a reference i.e. the MASS**. The range includes the analysis done in different seasons: summer and winter. The samples we are dealing about include 42 nights (summer) and 47 nights (winter). POD_1 is included in the range [48% - 69%] (slightly smaller than POD_3 but still very good) using as a reference the same instrument. Another not negligible favorable point for τ_0 is that this score of success has been obtained with just one model calibration (i.e. not a calibration for summer and one for winter) and we analyzed data in summer as well as in winter. It is highly probable that this score of success would further improve with a seasonal model calibration.

  The ability to detect a large τ_0 in advance is extremely useful for the following reasons. A large τ_0 permits an AO system to run at low temporal frequency and to use faint stars as a guide stars. A low temporal frequency permits indeed to better sample light coming from stars that, in presence of a smaller τ_0, can not be used as guide stars. A large τ_0 represents an advantage for the wide field AO because the number of available guide stars can, in genera,l increase and because a higher Strehl Ratio (SR) is reachable and more ambitious scientific projects can be carried out. The advantages are also for the classical SCAO configuration because it permits to observe fainter stars reaching a higher SR (see ANNEX B).

- The **total seeing (ε)** revealed to be sensitive to the seasonal model calibration. This means that the model needs a twofold calibration: one for summer and one for winter. We provided therefore in this study only the score of success for the summer time because the calibration sample belongs to this season. We will be able to use the measurements of the site testing campaign planned for Paranal with a Stereo-SCIDAR to calibrate the model for the winter time. In the case of the seeing, the most interesting POD from a scientific point of view is POD_1. **The probability to detect the $\varepsilon <$ 1" is in the range [62% - 72%]. The probability to detect the $\varepsilon <$ of the first tertile is in the range [48% - 53%].** The range in this case has the following meaning: the most conservative values (62% and 48% have been obtained with the sample of 42 nights (summer) in the 2010/2011 years. The most optimistic values have been obtained with the sub-sample of the 18 nights (summer) of 2007 (the same year in which the calibration sample belongs). The instrument used as a reference is the DIMM.

  The advantage in detecting in advance a weak ε is obvious. The best seeing conditions guarantee the highest SR of an AO system and the most challenging scientific programs such as the search and characterization of extra-solar planets would definitely gain from this condition.

- The **isoplanatic angle (θ_0)**, as the seeing, revealed to be sensitive to the seasonal model calibration. We provide therefore, in this study, only the score of success in summer for the same reason described for the seeing. From a scientific point of view, for θ_0 the most interesting POD is POD_3 that is the probability to detect a θ_0 larger than the third tertile. **POD_3 on the validation sample is equal to 58% when we considered as a reference the MASS**. The sample we are dealing about includes 21 nights (summer) of (2010/2011). No measurements with MASS are available for 2007. For completeness we also note that, at present, the probability to detect an isoplanatic angle smaller than the first tertile (POD_1) is not sufficiently good ($\sim$ 9%). This seems to come from the fact that the first tertile of Meso-Nh is slightly larger than that of measurements. We plan to undertake further investigations to improve this score of success. At the same time we highlight the fact that, from a scientific point of view, POD_3 is definitely more interesting than POD_1. We think therefore that at present, the system is clearly able to provide useful informations in terms of the Service Mode.

  A large value of the θ_0 is particularly useful for whatever kind of wide field AO (GLAO, MCAO, etc...). Observations supported by AO systems of extended and crowded fields such as clusters would definitely benefit from this condition if it would be known in advance.

- As an important example of the applications of our tool in Fig.73 - Fig.74 is reported the temporal evolution of the fraction of turbulence energy FTE in the first 600 m above the ground for a few nights of the PAR2007 site testing campaign as measured by the Generalized SCIDAR and as estimated by our tool (Astro-Meso-Nh package). It is well known that the temporal evolution of the FTE is crucial in the the Service Mode of scientific programs run on facilities assisted by AO systems, particularly Wide Field AO (WFAO) such as the AOF facility at Paranal.

To better put in evidence the correlation of the model with measurements Fig.75 shows the temporal evolution during eight different nights of the total seeing as reconstructed by the model (red line) and measured by the DIMM (black line). The green line indicates the DIMM measurements of the previous night. It is evident that the seeing reconstructed by the model well matches with the observed seeing.

HIGH VERTICAL RESOLUTION C_N^2 PROFILES

In this study we could also prove that, using a higher vertical resolution (173 levels instead of 62) of the Astro-Meso-Nh model it is possible to resolve many more layers in the C_N^2 profiles with a typical thickness that can reach the order of 150 m still covering the whole 20 km above the ground. Under these conditions, the temporal evolution of the seeing in the free atmosphere showed to have a consistent and realistic temporal variability. This is mainly thanks to the new algorithm of the C_N^2 and the fact that, since 2013, ECMWF products increased the number of vertical levels to 137 (instead of 91). This tells us that, provided the Meso-Nh model is calibrated for a specific vertical resolution, it might be used certainly to support AO systems of different typologies.

ARCHITECTURES AND COSTS

A detailed and extended analysis of different architectures has been carried out to find a good compromise between model performances, hardware performances and costs i.e. a good 'computing performances'/costs ratio that would permit to carry out within a fixed maximum threshold ΔT_{lim} forecasts of C_N^2 profiles and atmospherical parameters relevant for ground-based astronomy with model performances sufficiently high to guarantee a positive feedback in terms of Service Mode. **We achieved the fundamental goal to identify the suitable server at a cost of $\sim$ K€11**. The fact that Paranal and Armazones are just 22 km far away permits to save funds and to reduce the costs for setting-up a forecast system for the two astronomical sites. It is also important to note that, if in the future ESO would consider interesting to invest in forecasts of the C_N^2 at higher vertical resolution in the operational configuration, this can be possible but with a different architecture. This aspect was not part of this feasibility study but, considering the state of the art of the market, it might be realistic to envisage such a kind of forecast with reasonably limited costs.

WARNING FOR THE READER

Besides the report we provided as deliverables also a set of ppts, material presented in occasion of the milestones meetings and stored in the BSCW. For sake of readability of the report we decided to include in the report only those elements necessary to prove the key goals, basically a synthesis of the study. The rest of the material can be found in the BSCW. We cite for example, the temporal evolution of some parameters in all the nights under different data treatment (with or without moving average).

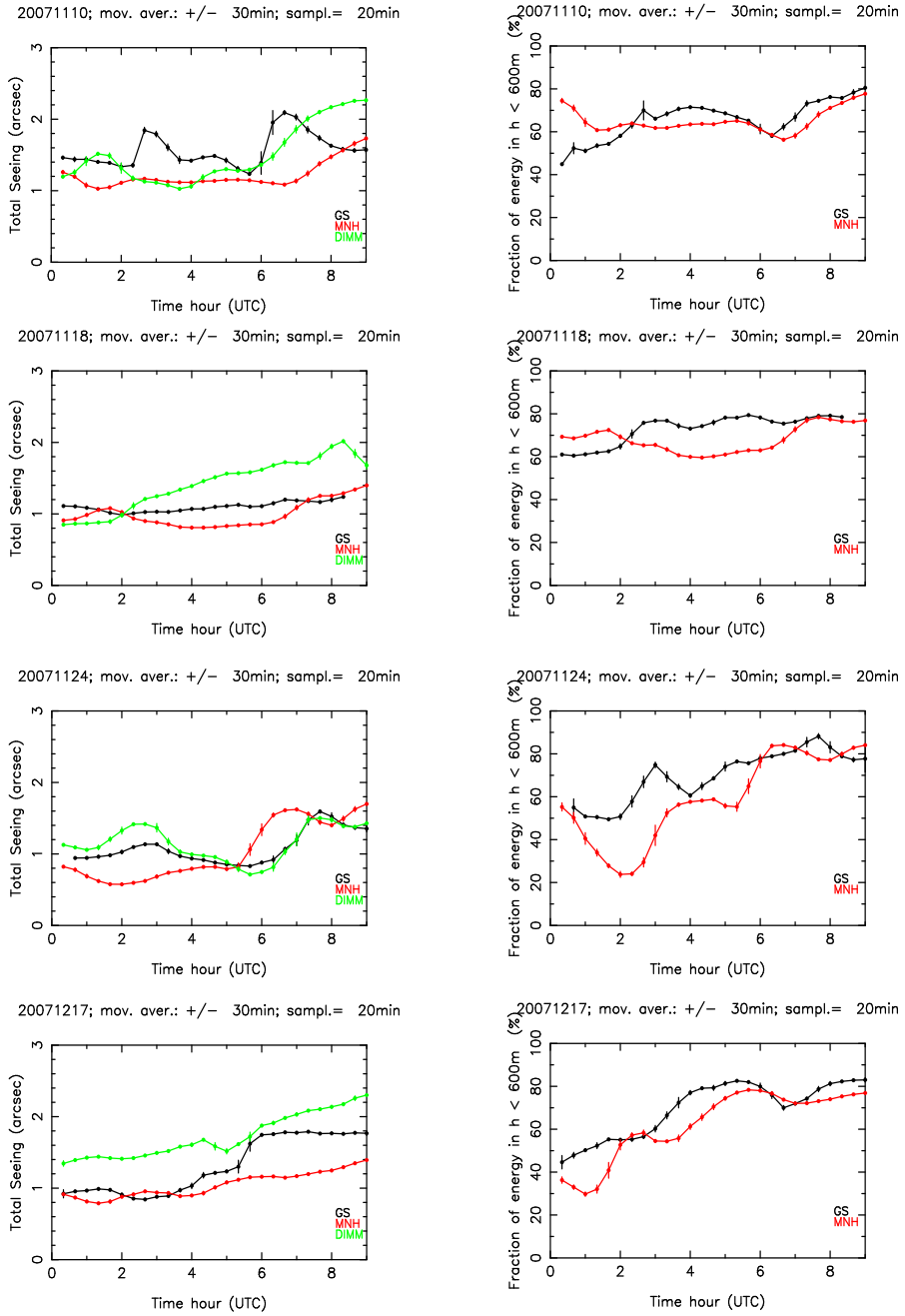

Figure 73: Left: temporal evolution of the total seeing as observed by DIMM (green line) and the Generalized SCIDAR (black line) and reconstructed by the Astro-Meso-nh model (red line). Right: temporal evolution of the fraction of the turbulence energy in the first 600 m as observed by the Generalized-SCIDAR (black line)and reconstructed by the model (red line).

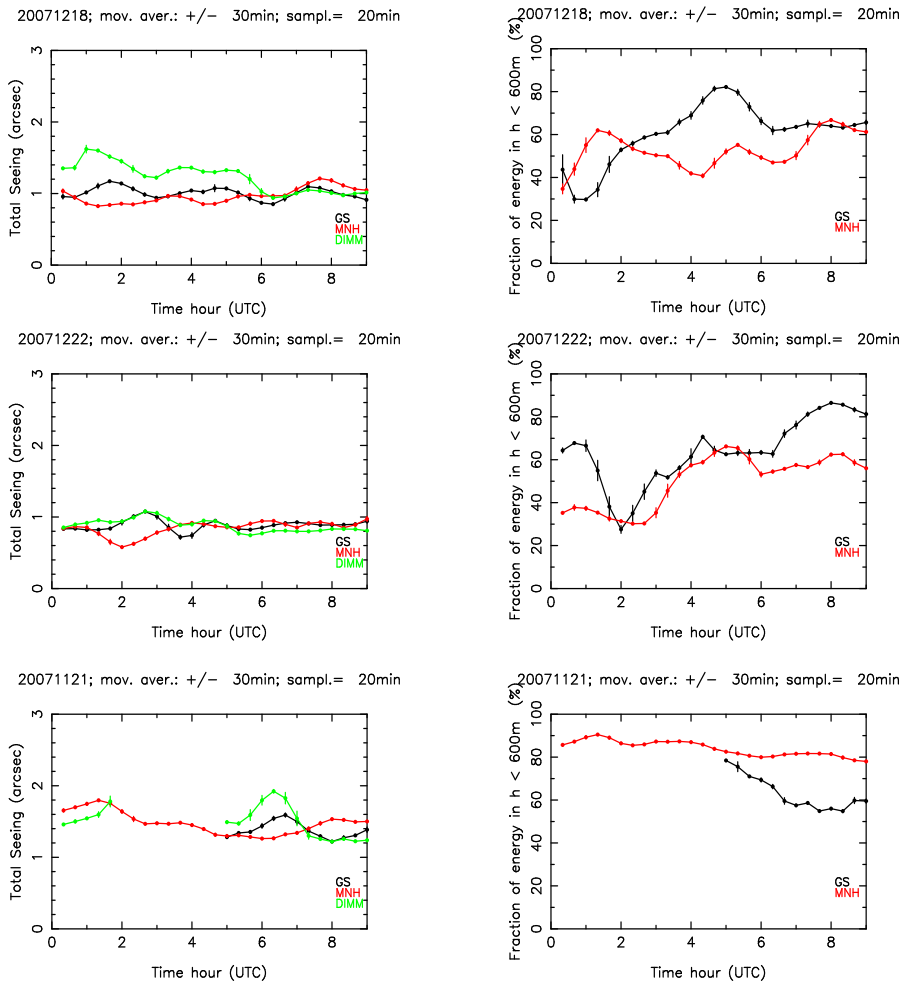

Figure 74: As for Fig.60.

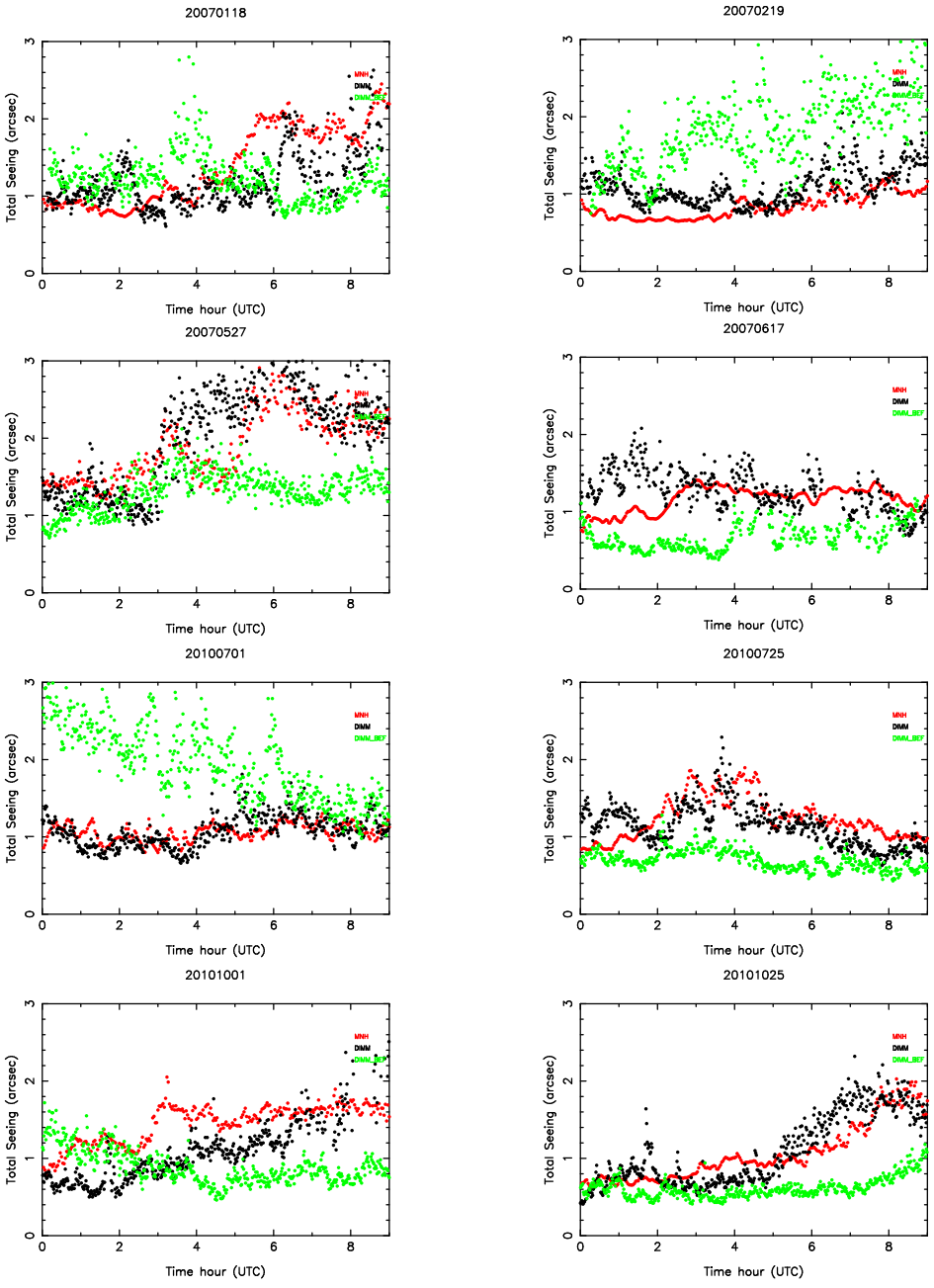

Figure 75: Temporal evolution of the total seeing as reconstructed by the model and observed by the DIMM (black line). The green line refers to the DIMM of the previous night.

11 MOSE Papers

List of papers published during the feasibility study (Phase A and Phase B). We planned at least one more paper in preparation for a peer-reviewed journal related to the model performances in predicting the OT and astroclimatic parameters.

Peer-Reviewed Journals

5. F. Lascaux, E. Masciadri and L. Fini, *Forecast of surface layer meteorological parameters at Cerro Paranal with a mesoscale atmospherical model*, MNRAS, 449, 1664, 2015

4. Masciadri, E., Lombardi, G., Lascaux, F., *On the comparison between MASS and generalized-SCIDAR techniques*, 2014, MNRAS, 438, 983

3. F. Lascaux, E. Masciadri and L. Fini, *MOSE: operational forecast of the optical turbulence and atmospherical parameters at European Southern Observatory ground-based sites - II atmospheric parameters in the surface layer 0-30m*, MNRAS, 436, 3147, 2013

2. E. Masciadri, F. Lascaux and L. Fini, *MOSE: operational forecast of the optical turbulence and atmospherical parameters at European Southern Observatory ground-based sites - I Overview and vertical stratification of atmospheric parameters at 0-20km*, MNRAS, 436, 1968, 2013

1. E. Masciadri, F. Lascaux, J. J. Fuensalida, G. Lombardi and H. Vasquez-Ramio, *Recalibrated generalized SCIDAR measurements at Cerro Paranal (the site of the Very Large Telescope)*, MNRAS, 420, 2399-24168, 2012

Non Peer-Reviewed Journals

7. E. Masciadri, F. Lascaux, L. Fini, *Dealing with the forecast of the optical turbulence as a tool to support astronomy assisted by AO facilities*, 2015, Journal of Physics: Conference Series, 595, id. 012020, DOI: 10.1088/1742-6596/595/1/012020

6. B. Neichel, E. Masciadri, A. Guesalaga, F. Lascaux, C. Béchet, *Towards a reliability assessment of the C_N^2 and wind speed vertical profiles retrieved from GeMS*, 2014 SPIE, 9148, id. 914863

5. Lascaux, F., Masciadri, E., Fini, L., *MOSE: verification of the Meso-Nh forecasts of the atmospheric surface parameters at Cerro Paranal and Cerro Armazones using contingency tables*; SPIE, 2014, id. 914865

4. Masciadri, E., Lascaux, F., Fini, L., *MOSE: a feasibility study for the prediction of the optical turbulence and meteorological parameters at Cerro Paranal and Cerro Armazones*, 2013, AO4ELT 3rd Edit., May 2013, DOI: 10.12839/AO4ELT3.13219

3. Lascaux, F., Masciadri, E., Fini, L., *MOSE: meso-scale prediction of near-ground meteorological parameters at ESO sites (Cerro Paranal and Cerro Armazones)*; AO4ELT3, 2013, DOI: 10.12839/AO4ELT3.13217

2. Masciadri, E., Lascaux, F., *MOSE: a feasibility study for optical turbulence forecast with the Meso-Nh model to support AO facilities at ESO sites (Paranal and Armazones)*; 2012, SPIE, 8447, id. 84475A

1. Lascaux, F., Masciadri, E., 2012, *MOSE: zooming on the Meso-Nh mesoscale model performances at the surface layer at ESO sites (Paranal and Armazones)*; SPIE, 8447, id. 84475B

ANNEX A

Simulated Nights - meteorological surface observations - Paranal				
2007-01-05	2007-01-18	2007-01-25	2007-02-05	2007-02-19
2007-02-25	2007-03-05	2007-03-15	2007-03-25	2007-04-05
2007-04-15	2007-04-27	2007-05-07	2007-05-15	2007-05-27
2007-06-07	2007-06-17	2007-06-27	2007-07-05	2007-07-15
2007-07-25	2007-08-05	2007-08-15	2007-08-25	2007-09-05
2007-09-15	2007-09-24	2007-10-05	2007-10-15	2007-10-25
2007-11-02	2007-11-03	2007-11-04	2007-11-05	2007-11-06
2007-11-07	2007-11-11	2007-11-13	2007-11-14	2007-11-15
2007-11-17	2007-11-18	2007-11-20	2007-11-25	2007-11-27
2007-11-28	2007-11-29	2007-11-30	2007-12-05	2007-12-14
2007-12-20	2007-12-22	2007-12-23	2007-12-24	2007-12-25
2010-06-02	2010-06-05	2010-06-08	2010-06-13	2010-06-17
2010-06-21	2010-06-26	2010-07-01	2010-07-05	2010-07-07
2010-07-10	2010-07-12	2010-07-15	2010-07-25	2010-07-29
2010-08-01	2010-08-02	2010-08-04	2010-08-05	2010-08-15
2010-08-20	2010-08-25	2010-08-31	2010-09-05	2010-09-13
2010-09-13	2010-09-15	2010-09-25	2010-10-01	2010-10-05
2010-10-17	2010-10-25	2010-10-31	2010-11-01	2010-11-05
2010-11-15	2010-11-25	2010-11-29	2010-12-02	2010-12-05
2010-12-13	2010-12-20	2010-12-25	2010-12-30	2011-01-02
2011-01-05	2011-01-15	2011-01-18	2011-01-22	2011-01-28
2011-01-31	2011-02-01	2011-02-05	2011-02-10	2011-02-15
2011-02-20	2011-02-24	2011-02-28	2011-03-03	2011-03-05
2011-03-10	2011-03-15	2011-03-20	2011-03-25	2011-03-31
2011-04-01	2011-04-05	2011-04-15	2011-04-25	2011-05-01
2011-05-05	2011-05-11	2011-05-15	2011-05-23	

Table 108: List of 129 simulated nights with available meteorological observations near the surface. These 129 nights were used for the validation of the model meteorological performances of Section 1 at Cerro Paranal, with both the ΔX = 500 m and ΔX = 100 m configurations.

Simulated Nights - meteorological surface observations - Paranal				
2010-05-16	2010-05-17	2010-05-29	2010-07-17	2010-09-02
2012-04-10	2012-04-13	2012-04-14	2013-02-06	2013-02-07
2013-05-18	2013-05-19	2013-08-25		

Table 109: List of 13 simulated nights with a strong observed relative humidity. These 13 nights were used for the validation of the model meteorological performances for the relative humidity of Section 1 at Cerro Paranal, with the ΔX = 500 m configuration.

Simulated Nights - meteorological surface observations - Armazones				
	2007-01-18	2007-01-25	2007-02-05	2007-02-19
2007-02-25	2007-03-05			
		2007-05-07		2007-05-27
		2007-06-27	2007-07-05	2007-07-15
2007-07-25		2007-08-15	2007-08-25	2007-09-05
2007-09-15	2007-09-24		2007-10-15	2007-10-25
2007-11-02	2007-11-03	2007-11-04	2007-11-05	2007-11-06
2007-11-07	2007-11-11	2007-11-13	2007-11-14	2007-11-15
2007-11-17	2007-11-18	2007-11-20	2007-11-25	2007-11-27
2007-11-28	2007-11-29	2007-11-30		2007-12-14
2007-12-20	2007-12-22	2007-12-23	2007-12-24	2007-12-25
2010-06-02	2010-06-05	2010-06-08	2010-06-13	2010-06-17
2010-06-21	2010-06-26	2010-07-01	2010-07-05	2010-07-07
2010-07-10			2010-07-25	2010-07-29
2010-08-01	2010-08-02	2010-08-04		2010-08-15
2010-08-20	2010-08-25	2010-08-31		
		2010-10-31	2010-11-01	2010-11-05
2010-11-15	2010-11-25	2010-11-29	2010-12-02	2010-12-05
2010-12-13	2010-12-20	2010-12-25	2010-12-30	2011-01-02
2011-01-05	2011-01-15	2011-01-18	2011-01-22	
2011-01-31	2011-02-01	2011-02-05	2011-02-10	2011-02-15
2011-02-20	2011-02-24	2011-02-28	2011-03-03	2011-03-05
2011-03-10	2011-03-15	2011-03-20	2011-03-25	2011-03-31

Table 110: List of simulated nights with available meteorological observations near the surface at Cerro Armazones (42 in 2007 (top) and 53 in 2010-2011 (bottom)). These 95 nights were used for the validation of the model meteorological performances of Section 1 at Cerro Armazones, with both the $\Delta X = 500$ m and $\Delta X = 100$ m configurations. They are a sub-sample of the 129 nights with observations at Cerro Paranal (cf. Table 108).

ANNEX B

Here we show a practical example in which the forecast of τ_0 might be determinant in the quality of observations. Fig.76 shows the SR in K and J band as a function of the τ_0 for different seeing conditions. Fig.77 shows the SR in K and J band as a function of the seeing ε for different τ_0 conditions.The simulations have been performed under the following conditions: Shack-Hartmann 40×40, sub-aperture FoV = 2.4", sampling frequency = 300 Hz, N. of corrected modes = 495, integrator gain = 0.6 and guide star with R magnitude 12. Looking at Fig.76 we observe that, for the same seeing, the SR can be more or less high depending on the value of τ_0. Looking at Fig.77 we observe that, the gain in SR is dramatic passing from 0.6" to 1.2" but the gain changes drastically for different values of τ_0.
Fig.78 shows the temporal evolution of the seeing and τ_0 during two different nights of the site testing campaign PAR2007 at Cerro Paranal (November/December 2007). The seeing in the two nights appears very similar and stable during the two nights. However, the τ_0 shows a consistent different value in the two nights. In spite of the fact that the seeing is mostly comparable during the two nights, one can expect a better SR in K band during the 21/12/2007 than during the 18/11/2007. Figure 78 is shown just to prove that this conditions can be realistic because these are real measurements of seeing and τ_0. Similar simulations might be done for different AO systems. It might be interesting for example, to calculate which might be the gain on AOF passing from 3 to 8 ms.

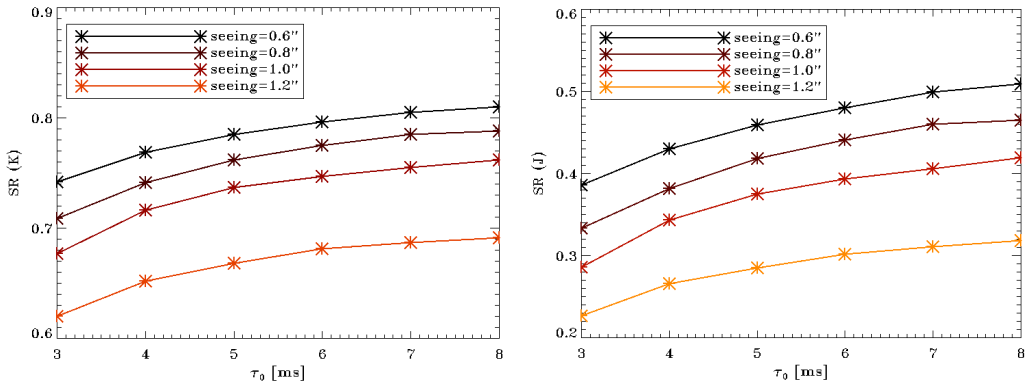

Figure 76: Temporal evolution of the SR in K band (left) and J band (right) as a function of the τ_0 for different values of the seeing (done by G. Agapito - Arcetri AO group - ERIS NGS AO)

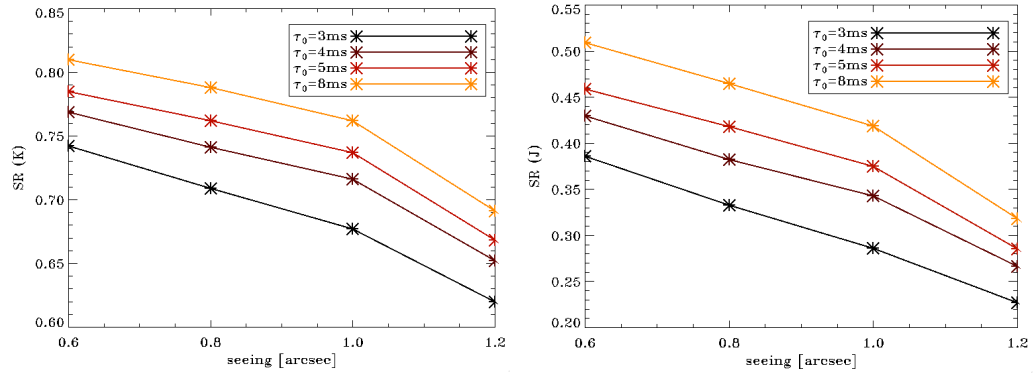

Figure 77: Temporal evolution of the SR in K band (left) and J band (right) as a function of the ε for different values of the τ_0 (done by G. Agapito - Arcetri AO group - ERIS NGS AO)

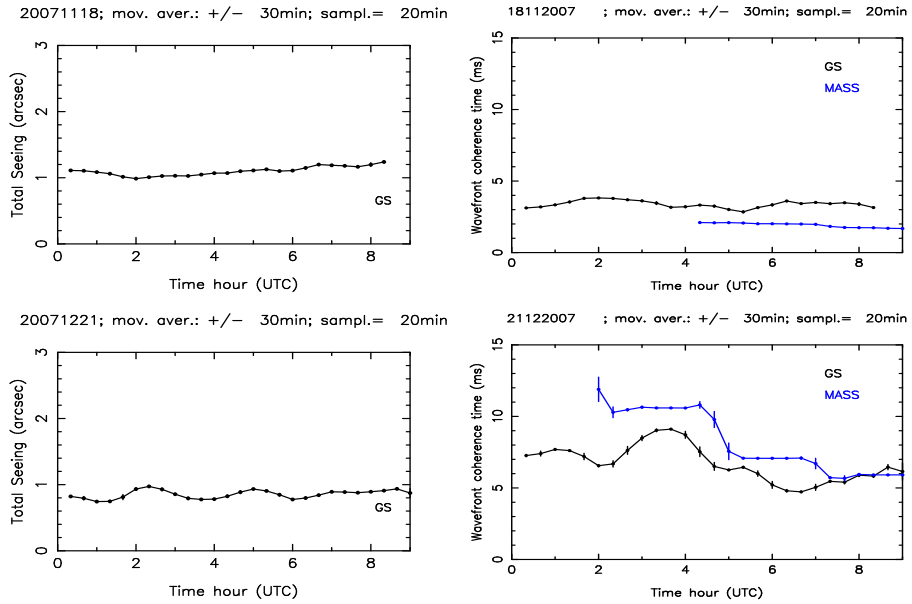

Figure 78: Temporal evolution of the seeing and the τ_0 in two different nights of the PAR2007 site testing campaign. Measurements from the GS and the MASS.

ANNEX C

In this Annex we report the results obtained by instruments and model on the sample of nights belonging to the PAR2007 site testing campaign (20 nights). Fig. 79 - Fig.83 show the C_N^2 temporal evolution measured by the Generalized SCIDAR and simulated by the model after the correction done with the coefficient A_1. Fig. 84 - Fig.88 show the C_N^2 temporal evolution simulated by the model in its standard configuration (before the correction with the coefficient A_1 and the coefficient A_1.

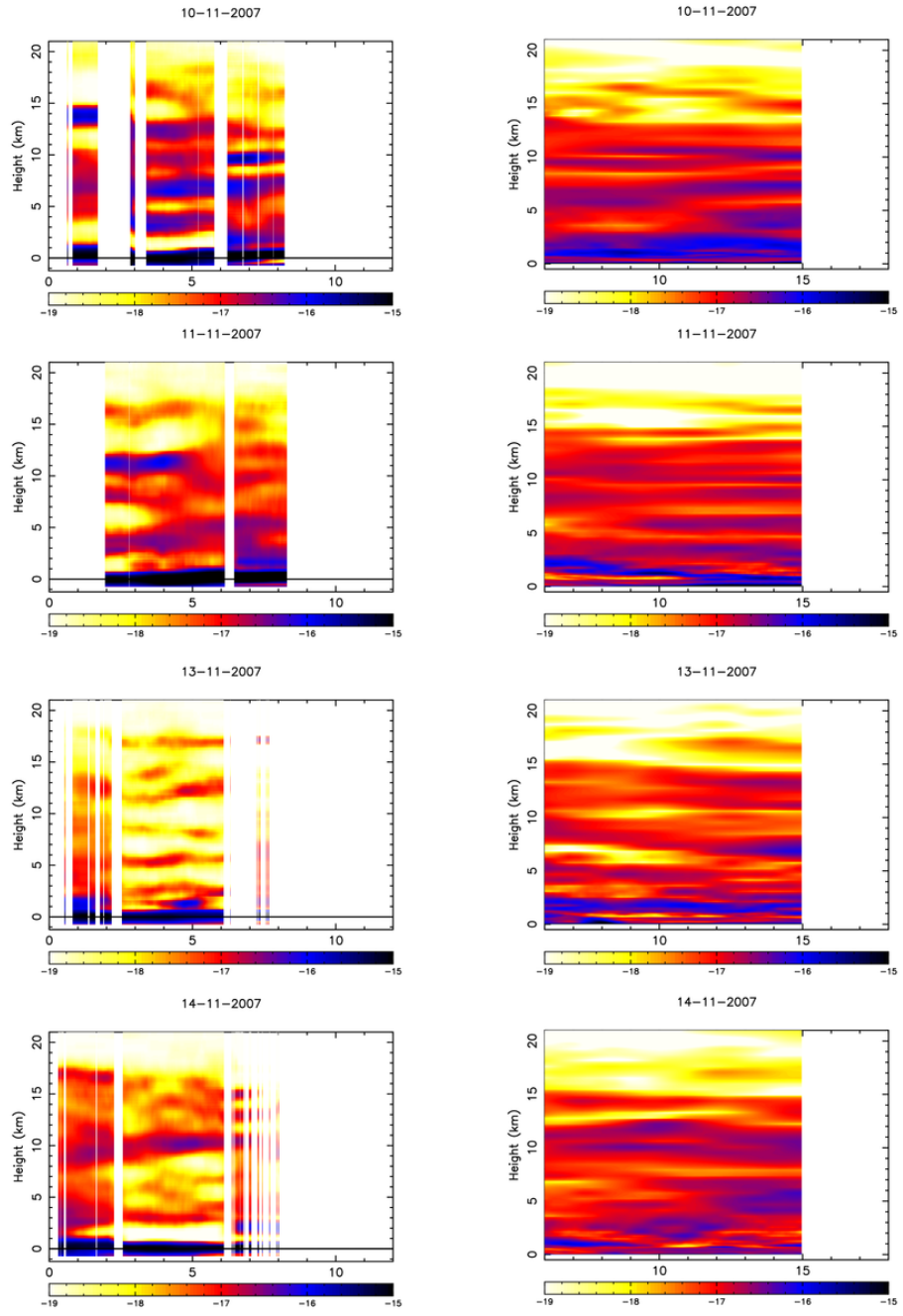

Figure 79: C_N^2 temporal evolution during the night. Left side: measurements provided by the Generalized SCIDAR. Right side: simulation provided by the model after the correction with the coefficient $A_1 1$ (see Section 5). The x-axis reports the time expressed in hours. For the image on the left side, these is time in UT therefore 00:00UT corresponds to 20:00 LT. For the image on the right side the hours correspond to the hours lasted from the beginning of the simulation (18:00UT of the day before). We have therefore that 06:00 corresponds to 20:00 LT. The two time cover therefore the same interval.

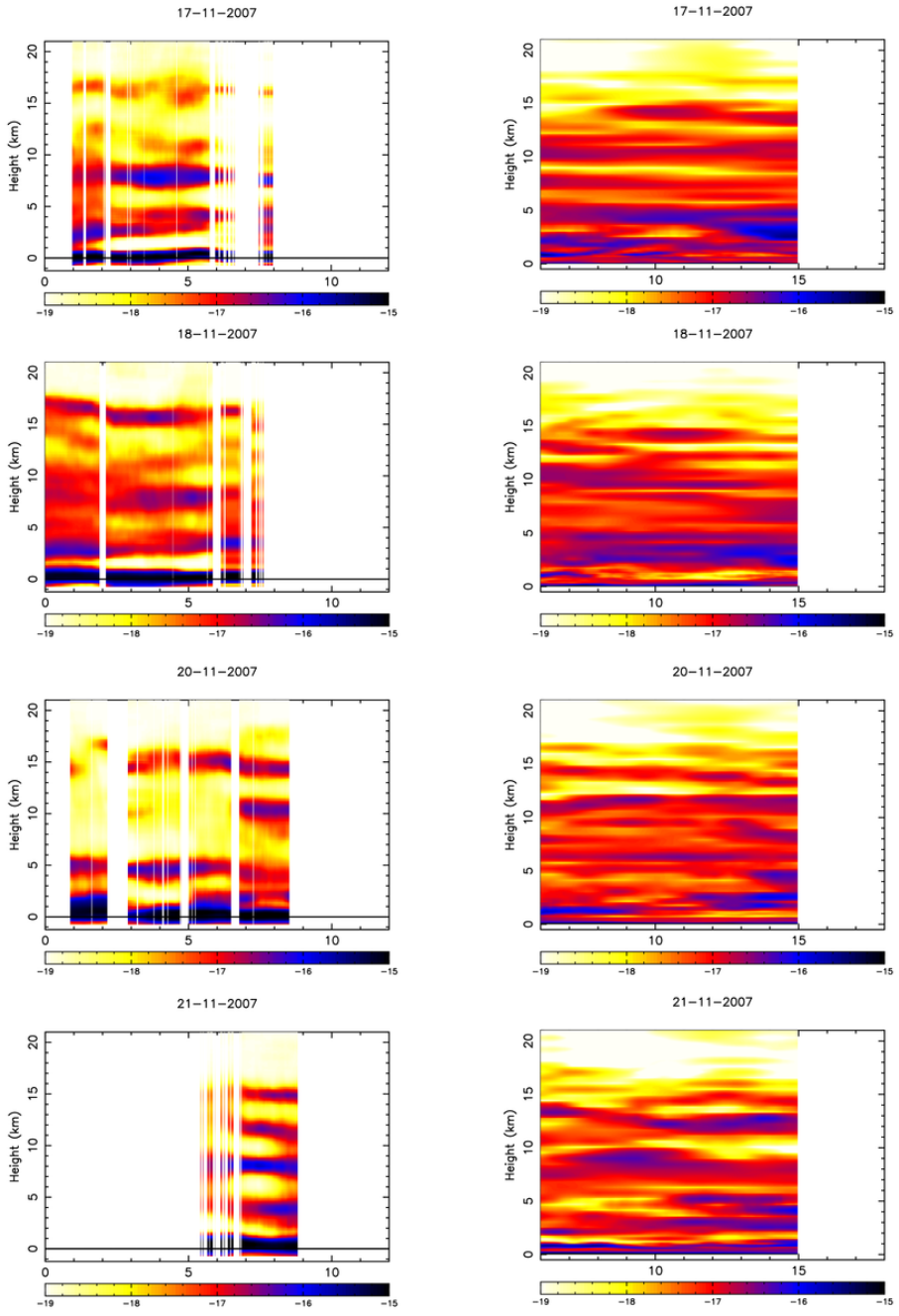

Figure 80: As Fig.79.

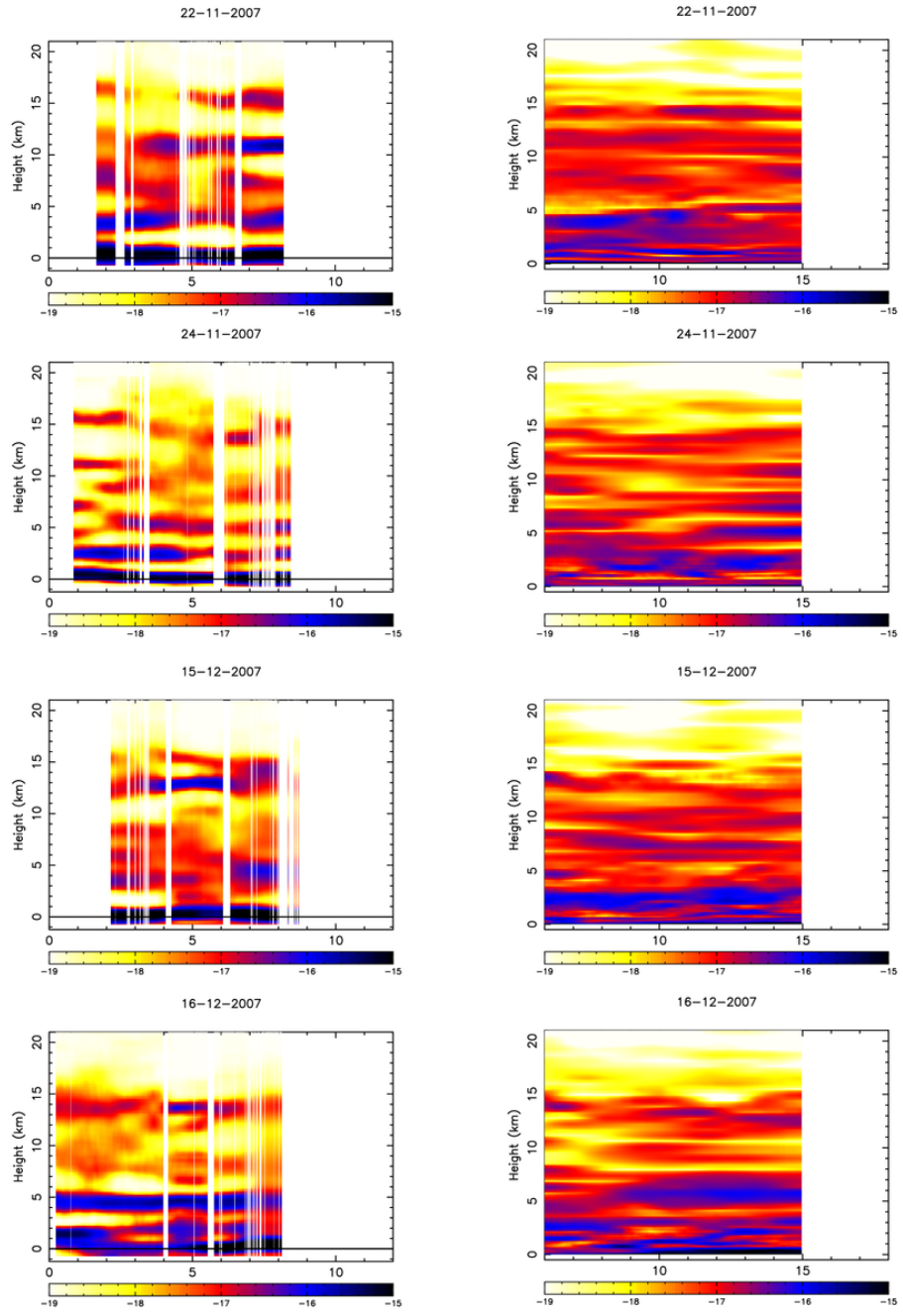

Figure 81: As Fig.79.

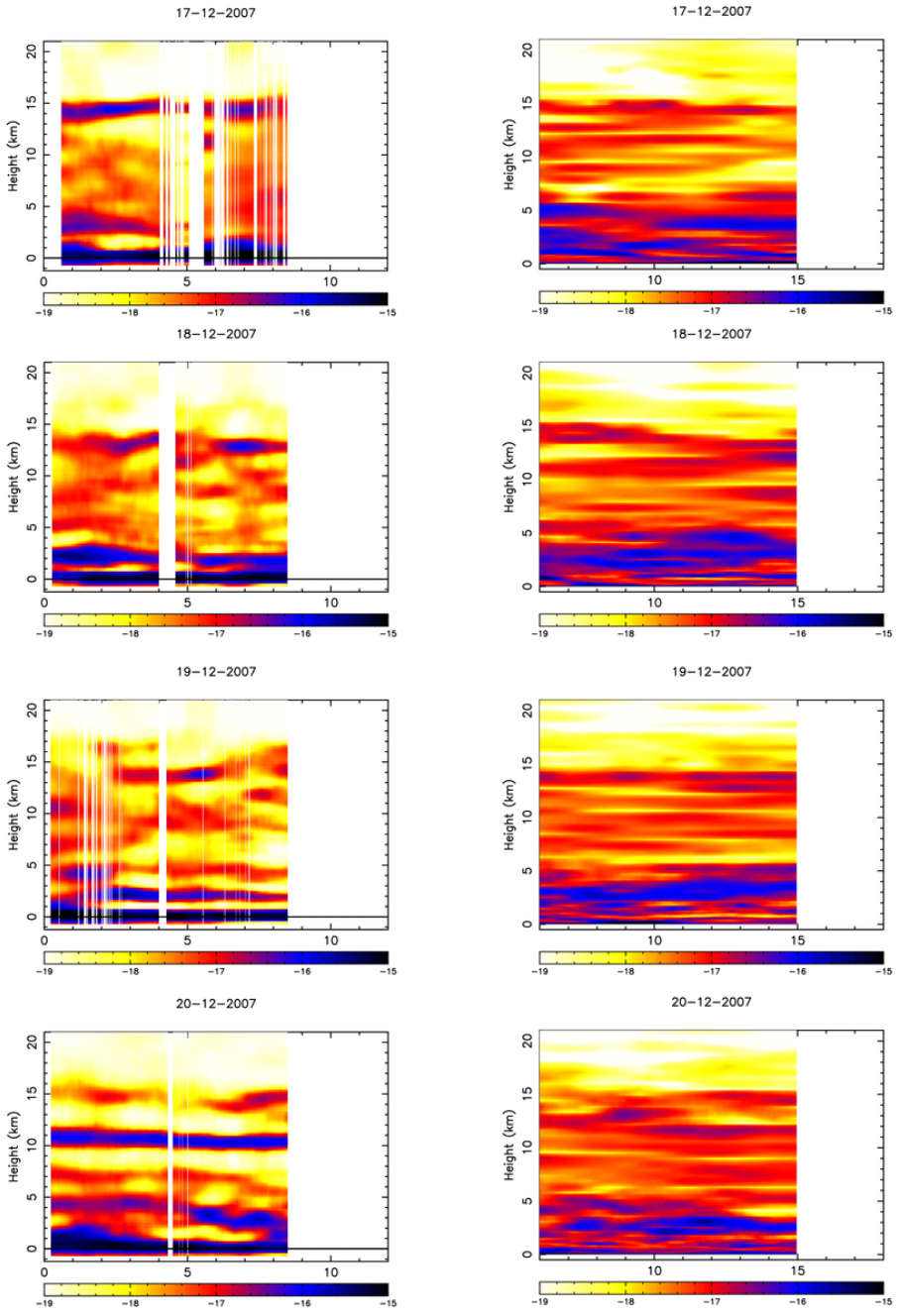

Figure 82: As Fig.79.

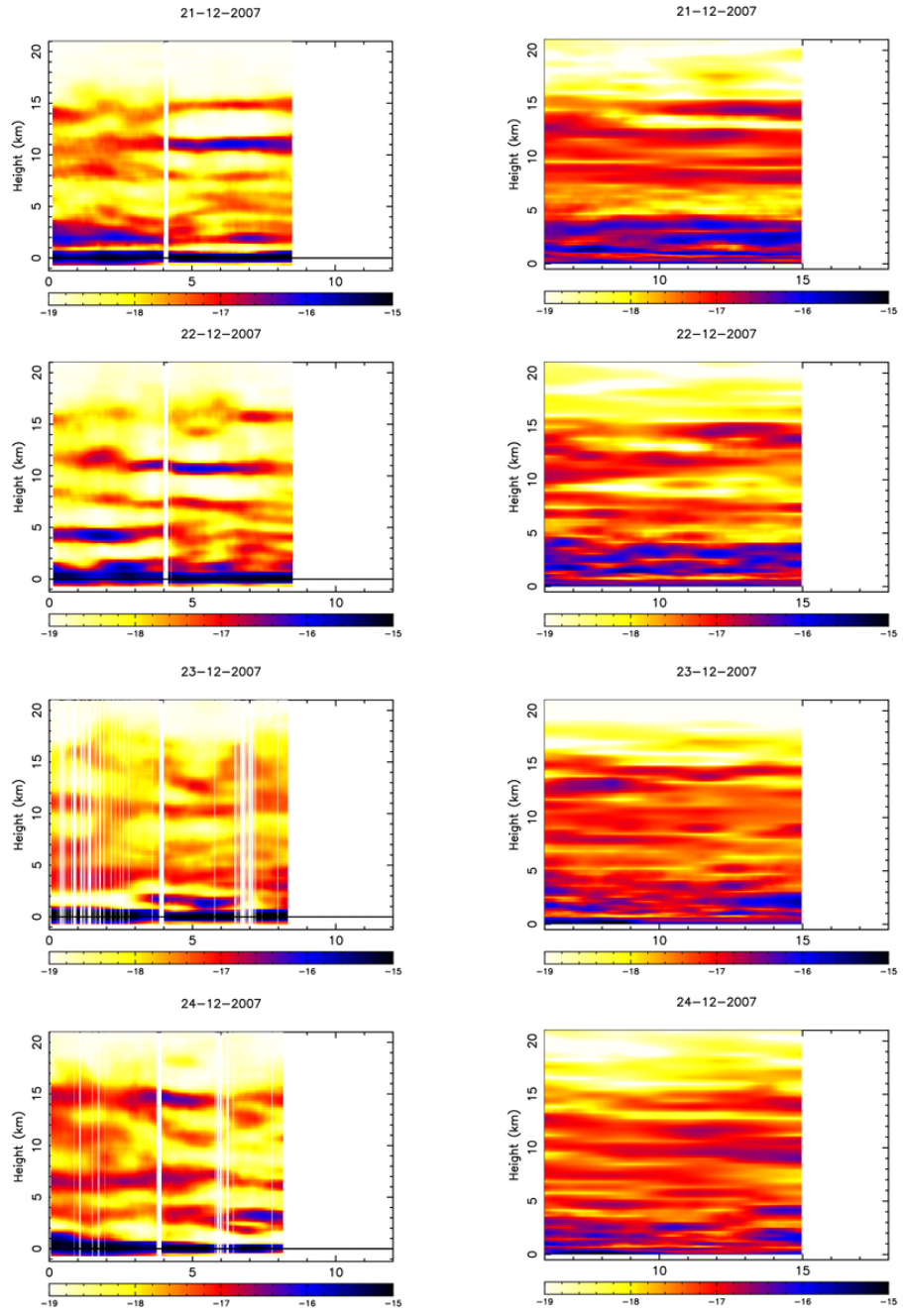

Figure 83: As Fig.79.

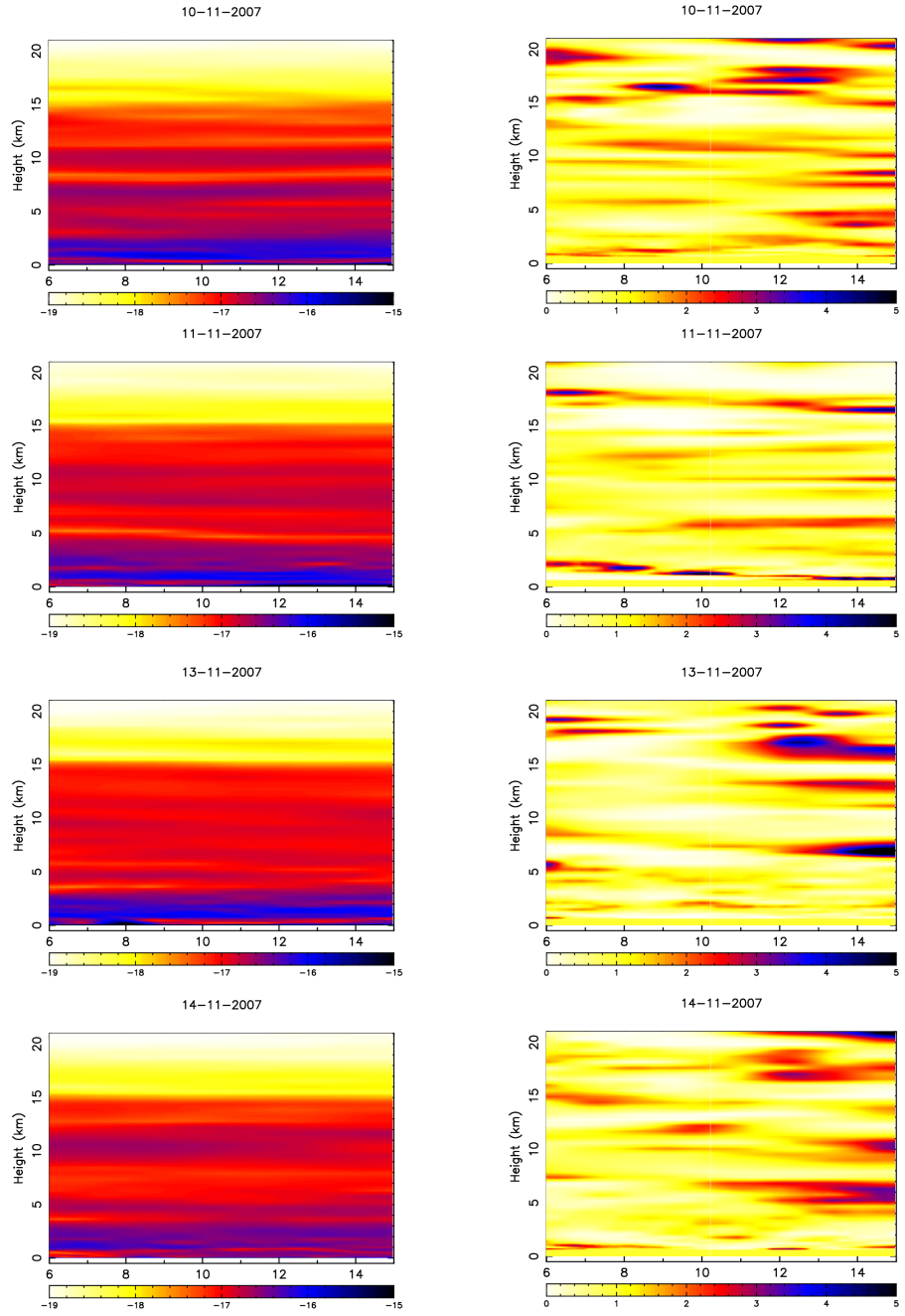

Figure 84: Left: C_N^2 temporal evolution during the whole night before the correction done with the coefficient A_1. Right: temporal evolution of the correction coefficient A_1. X-axis as Fig.79.

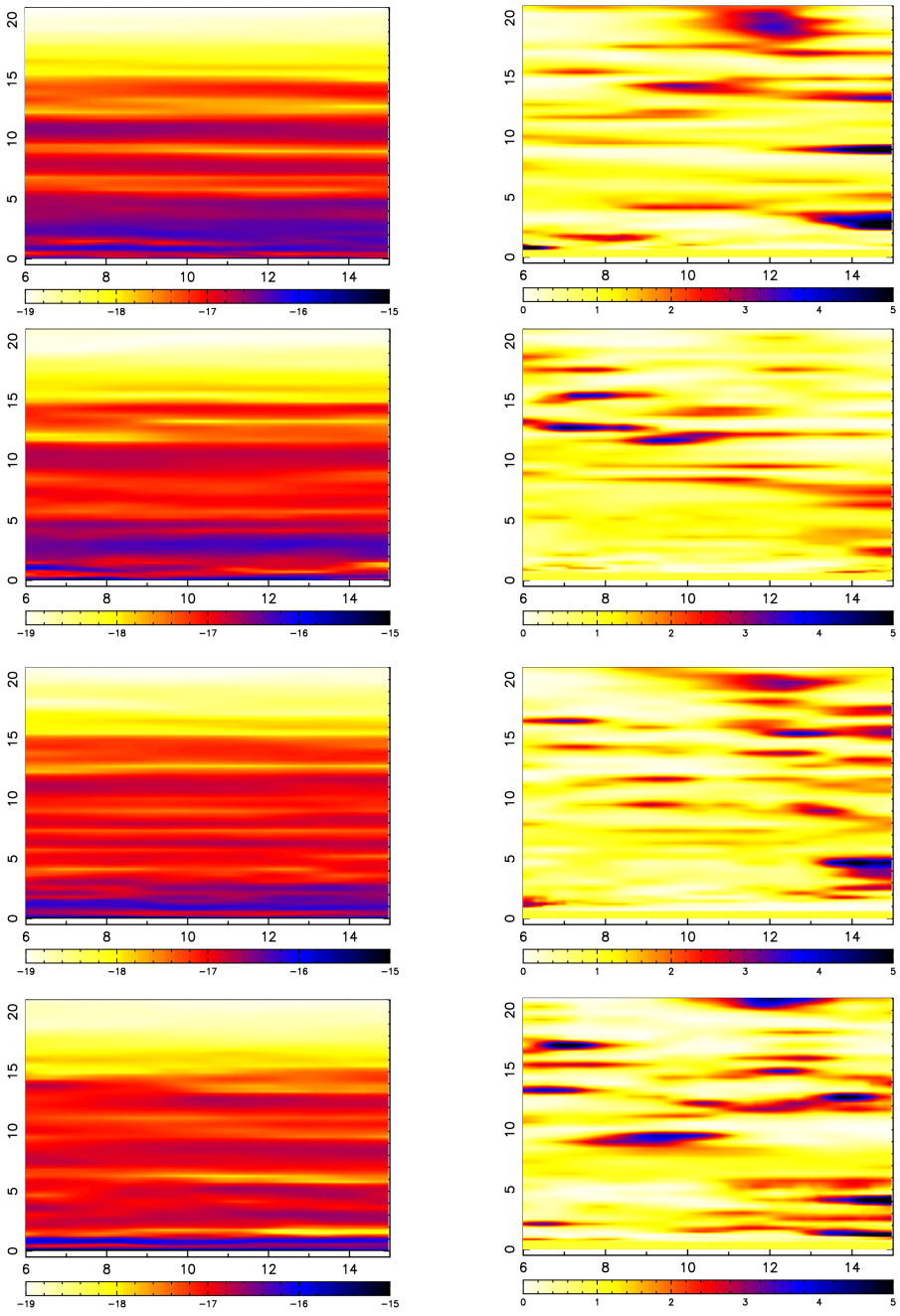

Figure 85: As Fig.84.

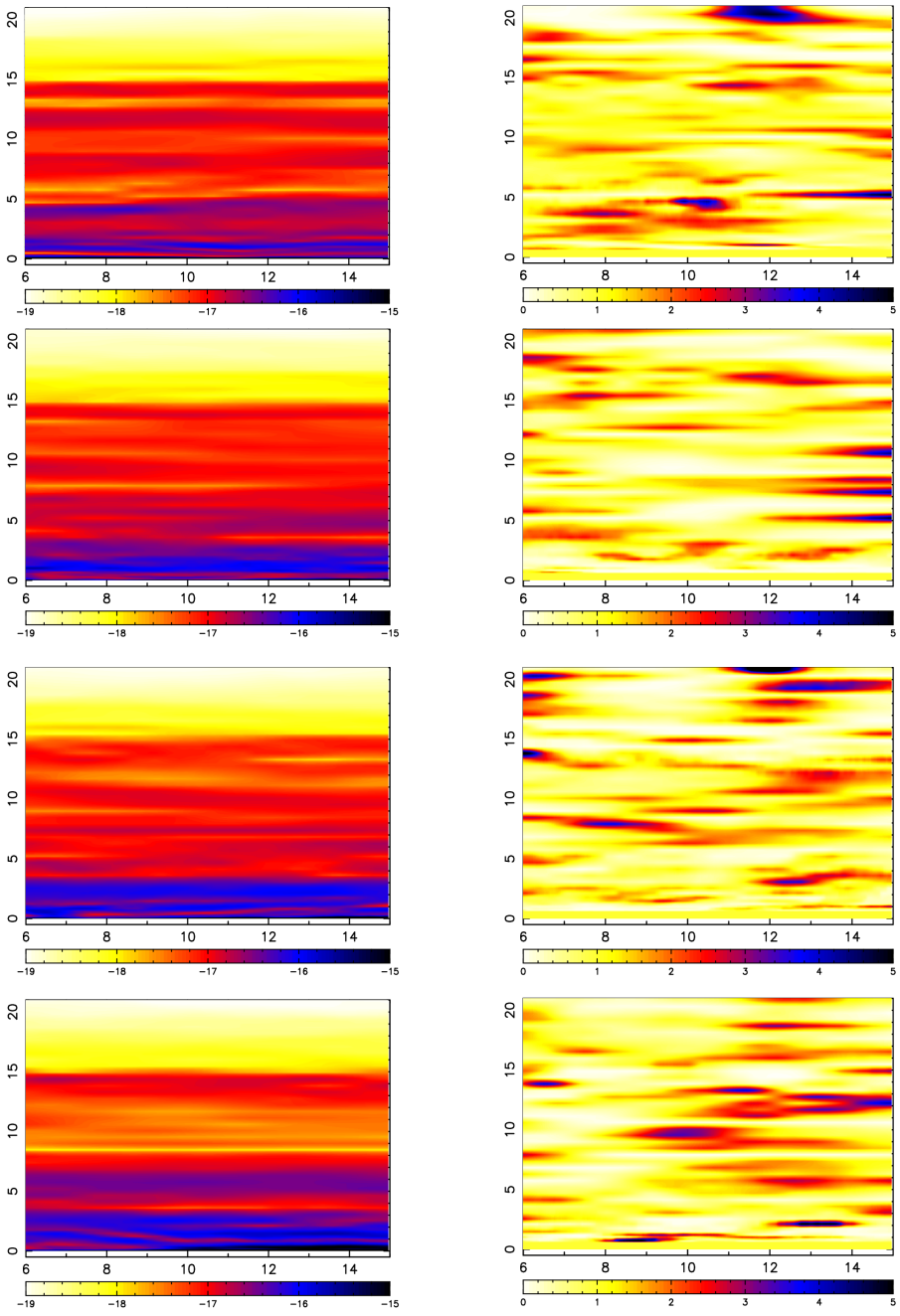

Figure 86: As Fig.84.

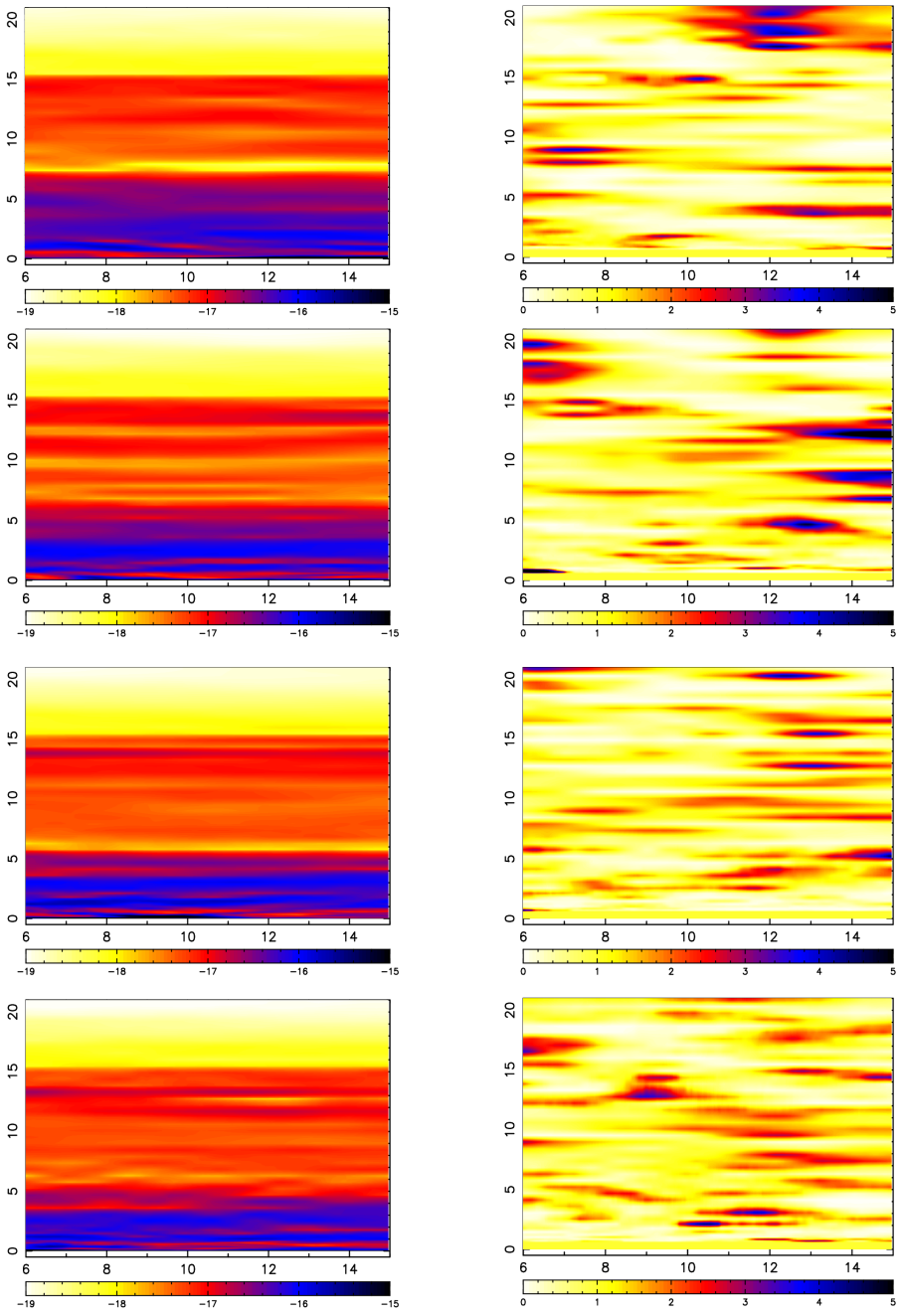

Figure 87: As Fig.84.

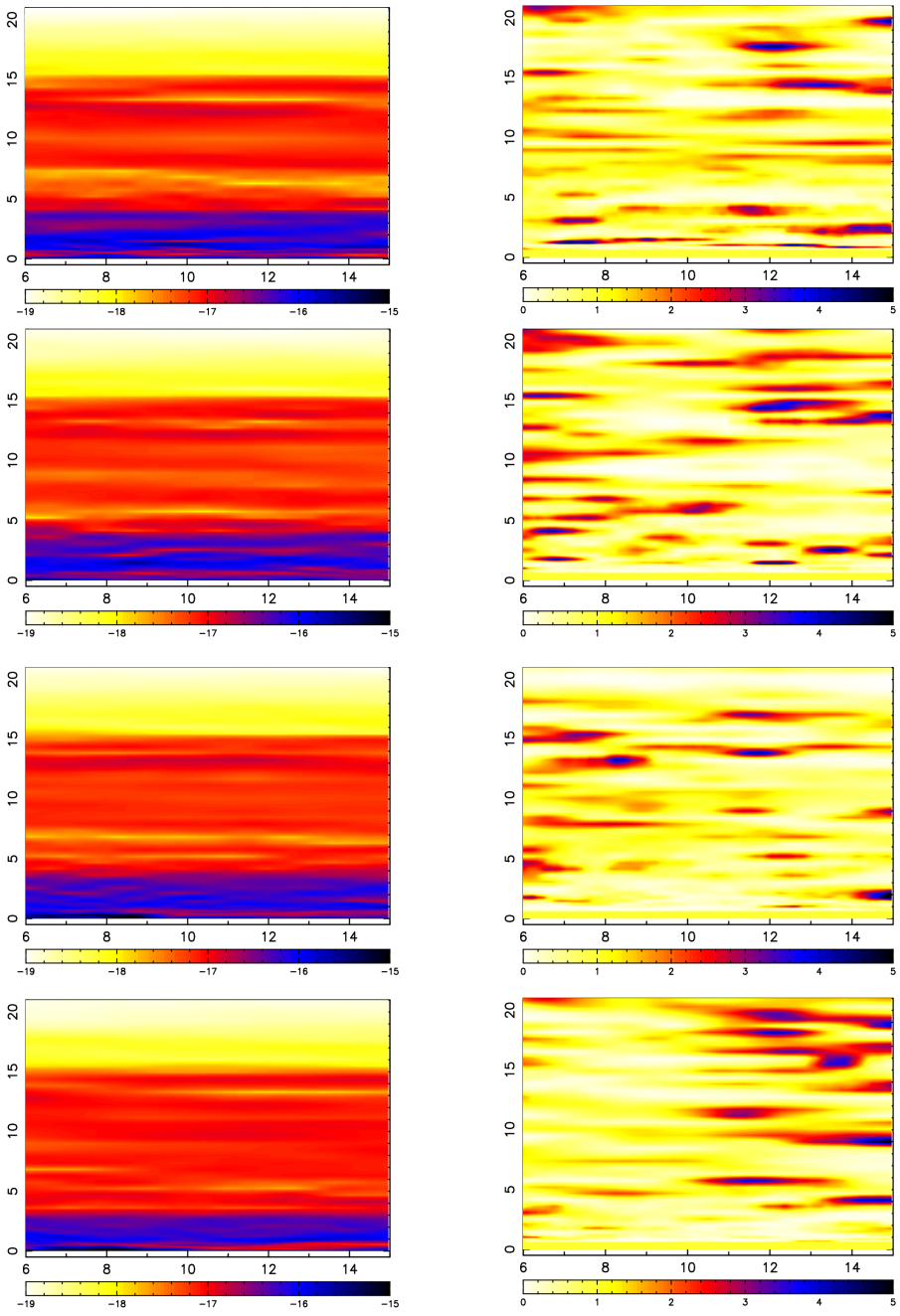

Figure 88: As Fig.84.

ACKNOWLEDGMENTS

Meteorological data-set from the Automatic Weather Station (AWS) and mast at Cerro Armazones are from the Thirty Meter Telescope Site Testing - Public Database Server [28]. Meteorological data-set from the AWS and mast at Cerro Paranal are from ESO Astronomical Site Monitor (ASM - Doc.N. VLT-MAN-ESO-17440-1773). We are very grateful to the whole staff of the TMT Site Testing Working Group for providing information about their data-set, to Marc Sarazin for his constant support to this study and for providing us the ESO data-set used in this study and to Florian Kerber for his valuable support in accessing at radio-soundings data-set. Radio-soundings have been launched and reduced by the M.Curé group of the Universidad de Valparaiso in the context of a study aiming to characterize the Precipitable Water Vapor (PWV) at Cerro Paranal. We acknowledge the whole ESO Board of MOSE for the useful suggestions and commentaries they kindly provided. Simulations are run partially on the HPCF cluster of the European Centre for Medium Weather Forecasts (ECMWF) - Project SPITFOT. This study is co-funded by the ESO contract: E-SOW-ESO-245-0933.

References

[1] E. Masciadri: *Optical Turbulence Modeling and Forecasts - Toward a new era for the ground-based astronomy*, Book Title: "Seeing Clearly: An Introduction to Atmospheric Optical Turbulence, its Measurement and Mitigation", Ed. S. Businger & T. Cherubini, Virtual Book Worm Publishing, pp. 131-164, 2011a.

[2] E. Masciadri, F. Lascaux and S. Hagelin: *Optical turbulence forecast with non-hydrostatical mesoscale models*, Second International Conference on Adaptive Optics for Extremely Large Telescopes, in Victoria, Canada. Online at http://ao4elt2.lesia.obspm.fr, id.79, 2011b.

[3] E. Masciadri, J. Vernin and P. Bougeault: *3D mapping of optical turbulence using an atmospheric numerical model. I. A useful tool for the ground-based astronomy*, A&ASS, 137, 185, 1999a

[4] R. Racine, D. Salmon, D. Cowley and J. Sovka: *Mirror, dome, and natural seeing at CFHT*, PASP, 1991, 103, 1020, 1991

[5] E. Masciadri and T. Garfias: *Wavefront coherence time season variability and forecasting at San Pedro Martir site*, A&A, 366, 708, 2001a

[6] E. Masciadri: *Near ground wind simulations by a meso-scale atmospherical model for the ELTs site selection*, RMxAA, 39, 249, 2003

[7] S. Hagelin, E. Masciadri and F. Lascaux: *Wind speed vertical distribution at Mt Graham*, MNRAS, 407, 2230, 2010

[8] E. Masciadri, J. Vernin and P. Bougeault, *3D mapping of optical turbulence using an atmospheric numerical model. II. First results at Cerro Paranal*, A&ASS, 137, 203, 1999b

[9] E. Masciadri and P. Jabouille, *Improvement in the Optical Turbulence Parametrization for 3D simulations in a region around a telescope*, A&A, 376, 727, 2001b

[10] E. Masciadri, R. Avila and L.J. Sanchez: *Statistic reliability of the Meso-Nh atmospherical model for 3D C_N^2 simulations*, RMxAA, 40, 3, 2004

[11] E. Masciadri and S. Egner: *First seasonal study of optical turbulence with an atmospheric model*, PASP, 118, 1604, 2006

[12] S. Hagelin, E. Masciadri and F. Lascaux: *Optical turbulence simulations at Mt Graham using the Meso-NH model*, MNRAS, 412, 2695, 2011

[13] F. Lascaux, E. Masciadri, J. Stoesz and S. Hagelin: *Mesoscale optical turbulence simulations at Dome C*, MNRAS, 398, 1093, 2009

[14] F. Lascaux, E. Masciadri and S. Hagelin: *Mesoscale optical turbulence simulations at Dome C: refinements*, MNRAS, 403, 1714, 2010

[15] F. Lascaux, E. Masciadri and S. Hagelin: *Mesoscale optical turbulence simulations above Dome C, Dome A and South Pole*, MNRAS, 411, 693, 2011

[16] J.-P. Lafore, J. Stein, N. Asencio, P. Bougeault, V. Ducrocq, J. Duron, C. Fischer, P. Hereil, P. Mascart, V. Masson, J.-P. Pinty, J.-L. Redelsperger, E. Richard and J. Vilà-Guerau de Arellano: *The Meso-NH Atmospheric Simulation System. Part I: adiabatic formulation and control simulations*, Annales Geophysicae, 16, 90, 1998

[17] T. Gal-Chen and C.J. Sommerville, "On the use of a coordinate transformation for the solution of the Navier-Stokes equations", *J. Comput. Phys.*, 17, pp. 209-228, 1975.

[18] A. Arakawa and F. Messinger, "Numerical methods used in atmospheric models", *GARP Tech. Rep.*, 17, WMO/ICSU, Geneva, Switzerland, 1976.

[19] R. Asselin, "Frequency filter for time integration", *Mon. Weather. Rev.*, 100, pp. 487-490, 1972.

[20] J. Cuxart, P. Bougeault and J.-L. Redelsperger, "A turbulence scheme allowing for mesoscale and large-eddy simulations", *Q. J. R. Meteorol. Soc.*, 126, pp. 1-30, 2000.

[21] P. Bougeault and P. Lacarrère, "Parameterization of orographic induced turbulence in a mesobeta scale model", *Mon. Weather. Rev.*, 117, pp. 1972-1890, 1989.

[22] J. Noilhan and S. Planton, "A simple paramterization of land surface processes for meteorological models", *Mon. Weather. Rev.*, 117, pp. 536-549, 1989.

[23] E. Masciadri, J. Vernin and P. Bougeault, *3D numerical simulation of optical turbulence at Roque de Los Muchachos Observatory using the atmospherical model Meso-Nh*, A&A, 365, 699, 2001c

[24] E. Masciadri, R. Avila and L.J. Sanchez: *First evidence of the finite horizontal extent of the optical turbulence layers. Implications for the new adaptive optics techniques*, A&A , 382, 387, 2002

[25] J. Stein, E. Richard, J.-P. Lafore, J.-P. Pinty., N. Asencio and S. Cosma, "High-Resolution Non-Hydrostatic Simulations of Flash-Flood Episodes with Grid-Nesting and Ice-Phase Parameterization", *Meteorol. Atmos. Phys.*, 72, pp. 203-221, 2000.

[26] A. Chácon, O. Cuevas, D. Pozo, J. Marìn, A. Oyanadel, C. Dougnac, L. Cortes, L. Illanes, M. Caneo, M. Curé, M. Sarazin, F. Kerber, A. Smette, D. Rabanus, R. Querel and G. Tompkins, *Measuring and forecasting of PWV above La Silla, APEX and Paranal Observatories*, RMxAC, 41, 20-23, 2011

[27] S. Sandrock and R. Amestica, *VLT Astronomical Site Monitor - ASM Data User Manual*, Doc no.: VLT-MAN-ESO-17440-1773, 1999

[28] M. Schoeck, S. Els, R. Riddle, W. Skidmore, T. Travouillon, R. Blum, E. Bustos, G. Chanan, S. G. Djorgovski, P. Gillett, B. Gregory, J. Nelson, A. Otárola, A. Seguel, J. Vasquez, J. Walker, A. Walker, and D. Wang, ,*Thirty Meter Telescope Site Testing I: Overview*, PASP, 121, 384-395, 2009

[29] W. Skidmore, T. Travouillon and R. Riddle, *Report of the calibration of the T2-Armazones, 30-m tower air temperature sensors and sonic anemometers, the cross comparison of weather stations and sonic anemometers and turbulence measurements of sonic anemometers and finewire thermocouples*, Internal TMT Report, 2007

[30] N. I. Fisher and A. J. Lee, *A Correlation Coefficient for Circular Data*, Biometrika, 70, 327-332, 1983

[31] E. Masciadri, F. Lascaux, J. J. Fuensalida, G. Lombardi and H. Vasquez-Ramio, *Recalibrated generalized SCIDAR measurements at Cerro Paranal (the site of the Very Large Telescope)*, MNRAS, 420, 2399-24168, 2012

[32] R. A. Johnston, C. Dainty, N. J. Wooder, R. G. Lane, *Generalized scintillation detection and ranging results obtained by use of a modified inversion technique*, App. Optics, 41, 6788-6772, 2002

[33] R. Avila and S. Cuevas, *On the normalization of scintillation autocovariance for generalized SCIDAR*, Optics Express, 17, 3, p. 10926, 2009

[34] V. Kornilov, *Stellar scintillation in the short exposure regime and atmospheric coherence time evaluation*, A&A, 530, id.A56, 7 pp., 2011

[35] W. Dali Ali, A. Ziad, A. Berdja, J. Maire, J. Borgnino, M. Sarazin, G. Lombardi, J. Navarrete, H. Vazquez Ramio, M. Reyes, J. M. Delgado, J. J. Fuensalida, A. Tokovinin and E. Bustos, *Multi-instrument measurement campaign at Paranal in 2007 - Characterization of the outer scale and the seeing of the surface layer*, A&A, 524, id.A73, 8 pp., 2010

[36] E. Masciadri, J. Stoesz, S. Hagelin and F. Lascaux, *Optical turbulence vertical distribution with standard and high resolution at Mt Graham*, MNRAS, 404, 144-158, 2010

[37] M. Chun, R. Wilson, R. Avila, T. Butterley, J.-L. Aviles, D. Wier and D. Benigni, *Mauna Kea ground-layer characterization campaign*, MNRA, 394, 1121-1130, 2009

[38] H. Vazquez-Ramio, J. Vernin, C. Munoz-Tunon, M. Sarazin, A. M. Varela, H. Trinquet, J. M. Delgado, J. J. Fuensalida, M. Reyes, A. Benhida, Z. Benkhaldoun, D. G. Lambas, Y. Hach, M. Lazrek, G. Lombardi, J. Navarrete, P. Recabarren, V. Renzi, M.Sabil and R. Vrech, *European Extremely Large Telescope Site Characterization. II. High Angular Resolution Parameters*, 124, 918, 868-884, 2012

[39] J.E. Thomas-Osip, G. Prieto, A. Berdja, K.W. Cook, S. Villanueva, Jr., D.L. DePoy, J.L. Marshall, J.P. Rheault, R.D. Allen, D.W. Carona, CHaracterizing Optical turbulence at the GMT site with MooSci and MASS-DIMM, PASP, 124, 84, 2012

[40] M. Sarazin & A. Tokovinin, *The Statistics of Isoplanatic Angle and Adaptive Optics Time Constant derived from DIMM Data*, ESO Conference and Workshop Proceedings, 58, 321-328, 2002

[41] Avila, R., Vernin, J., Cuevas, S., *Turbulences profiles with Generalized Scidar at San Pedro Mártir Observatory and isoplanatic study*, PASP, 110, 1106, 1998

[42] J. Krause-Polstorff, A. Edmund, and L. W. Donald, *Instrument comparison: corrected stellar scintillometer versus isoplanometer*, Appl. Opt. 32, 40514057, 1993

[43] A. Ziad, R. Conan, A. Tokovini, F. Martin and J. Borgnino, *From the Grating Scale Monitor to the Generalized Seeing Monitor*, App. Opt., 39, 5415-5425, 2000

[44] Nurmi, P., *Recommendations on the verification of local weather forecasts (at ECMWF Member States) - Consultancy Report (ECMWF Operations Department)*, 2003

[45] Thornes, J.E., Stephenson. D.B., *How to judge the quality and value of weather forecast products*, Meteorol. Appl., 8, 307, 2001

[46] T. Fusco, G. Rousset, D. Rabaud, E. Gendron D. Mouillet, F. Lacombe, G. Zins, P.-Y. Madec, A.-M. Lagrange, J. Charton, D. Rouan, N. Hubin and N. Ageorges, *NAOS on-line characterization of turbulence parameters and adaptive optics performance*, J, Opt. A., 6, 585-596, 2004

[47] J. Kolb, N. Muller, E. Aller-Carpentier, P. Andrade and J. Girard, *What can be retrieved from Adaptive Optics real-time data?*, Proc. of SPIE: Adaptive Optics Systems III, 8447, 84475U, 2012

[48] J. Kolb, *Turbulence characterization at the Nasmyth focal plane of the VLT Melipal*, Proc. of SPIE: Adaptive Optics Systems.7015, 70154O, 2008

[49] P. Martinez, J. Kolb, M. Sarazin, J. Navarrete, *Active optics Shack-Hartmann sensor: using spot sizes to measure the seeing at the focal plane of a telescope*, MNRAS, 421, 3019-3026, 2012

[50] E.Masciadri, G.Rousset, T.Fusco, P.Bonifacio, J.Fuensalida, C.Robert, M.Sarazin, R.Wilson, A.Ziad, A roadmap for a new era turbulence studies program applied to the ground-based astronomy supported by AO, AO4ELT 3rd Edit., Florence 27-31 May, 2013

[51] E. Masciadri, F. Lascaux and L. Fini, *MOSE: operational forecast of the optical turbulence and atmospherical parameters at European Southern Observatory ground-based sites - I Overview and vertical stratification of atmospheric parameters at 0-20km*, MNRAS, 436, 1968, 2013

[52] F. Lascaux, E. Masciadri and L. Fini, *MOSE: operational forecast of the optical turbulence and atmospherical parameters at European Southern Observatory ground-based sites - II atmospheric parameters in the surface layer 0-30m*, MNRAS, 436, 3147, 2013

[53] F. Lascaux, E. Masciadri and L. Fini, *Forecast of surface layer meteorological parameters at Cerro Paranal with a mesoscale atmospherical model*, MNRAS, 449, 1664, 2015

[54] Masciadri, E., Lombardi, G., Lascaux, F., *On the comparison between MASS and generalized-SCIDAR techniques*, 2014, MNRAS, 438, 983

[55] Masciadri, E., Lascaux, F., Fini, L., *MOSE: a feasibility study for the prediction of the optical turbulence and meteorological parameters at Cerro Paranal and Cerro Armazones*, 2013, AO4ELT 3rd Edit., May 2013, DOI: 10.12839/AO4ELT3.13219

[56] B. Neichel, E. Masciadri, A. Guesalaga, F. Lascaux, C. Béchet, *Towards a reliability assessment of the C_N^2 and wind speed vertical profiles retrieved from GeMS*, 2014 SPIE, 9148, id. 914863

[57] E. Masciadri, F. Lascaux, L. Fini, *Dealing with the forecast of the optical turbulence as a tool to support astronomy assisted by AO facilities*, 2015, Journal of Physics: Conference Series, 595, id. 012020, DOI: 10.1088/1742-6596/595/1/012020